

PROPAGATION OF NEUTRON WAVES
THROUGH HETEROGENEOUS MULTIPLYING
AND NONMULTIPLYING MEDIA

By

VICTOR RALPH CAIN

A DISSERTATION PRESENTED TO THE GRADUATE COUNCIL OF
THE UNIVERSITY OF FLORIDA
IN PARTIAL FULFILLMENT OF THE REQUIREMENTS FOR THE
DEGREE OF DOCTOR OF PHILOSOPHY

UNIVERSITY OF FLORIDA

August, 1965



UNIVERSITY OF FLORIDA



3 1262 08552 5383

To Bliz

ACKNOWLEDGMENTS

The author wishes to express his appreciation to his supervisory committee for their assistance. Special appreciation is due to the committee chairman, Dr. Rafael Perez, for his unusual patience and constant encouragement and guidance.

Acknowledgment must also be rendered to the Department of Nuclear Engineering and to the Computing Center of the University of Florida for their combined financial support of the computational work for this dissertation.

Finally, the author wishes to acknowledge his debt to the Oak Ridge National Laboratory and to the U.S. Atomic Energy Commission for the assignment which made this work possible.

TABLE OF CONTENTS

	PAGE
ACKNOWLEDGMENTS	iii
LIST OF FIGURES	v
ABSTRACT	vii
INTRODUCTION	1
CHAPTER I. USE OF A ONE-GROUP ONE-DIMENSIONAL GREEN'S FUNCTION IN HETEROGENEOUS MEDIA	4
II. USE OF A ONE-GROUP TWO-DIMENSIONAL GREEN'S FUNCTION IN HETEROGENEOUS MEDIA	21
III. USE OF AN AGE-DIFFUSION TWO-DIMENSIONAL GREEN'S FUNCTION IN HETEROGENEOUS MEDIA	30
IV. CALCULATIONAL RESULTS	58
V. SUMMARY AND CONCLUSIONS	79
APPENDICES	
A. The Complex Arithmetic Version of GINV	88
B. Digital Computer Techniques for the Calculation of the Error Function with a Complex Argument	93
C. Galanin's Thermal Constant for a Sinusoidally Varying Flux	101
D. Physical Constants Used in Sample Calculations	103
REFERENCES	104

LIST OF FIGURES

FIGURE	PAGE
1. Geometry for the One-Group, One-Dimension Green's Function Calculation	5
2. One-Group Flux Amplitude <u>vs</u> Distance Along the Z Axis for One Cadmium Foil in Graphite, at 100 cps, with 1, 2, 4, and 10 Spatial Modes	66
3. One-Group Flux Amplitude <u>vs</u> Distance Along the Z Axis for One Cadmium Foil in Graphite, at 1000 cps, with 1, 2, 4, and 10 Spatial Modes	67
4. One-Group Flux Phase Lag <u>vs</u> Distance Along the Z Axis for One Cadmium Foil in Graphite, at 100 cps, with 1, 2, 4, and 10 Spatial Modes	68
5. One-Group Flux Phase Lag <u>vs</u> Distance Along the Z Axis for One Cadmium Foil in Graphite, at 1000 cps, with 1, 2, 4, and 10 Spatial Modes	69
6. Flux Amplitude <u>vs</u> Distance Along the Z Axis for Two Cadmium or Uranium Foils in Graphite, at 200, 500, and 800 cps, with One Spatial Mode	71
7. Flux Amplitude <u>vs</u> Distance Along the Z Axis for Two Cadmium or Uranium Foils in Graphite, at 200, 500, and 800 cps, with Six Spatial Modes	72
8. Flux Phase Lag <u>vs</u> Distance Along the Z Axis for Two Cadmium or Uranium Foils in Graphite, at 200, 500, and 800 cps, with One and Six Spatial Modes	73
9. One-Group Flux Amplitude <u>vs</u> Source Frequency for Two Cadmium Foils in Graphite, at $z = 2, 8, 8.89, 15$, and 30 cm, with Six Spatial Modes	74

10. One-Group Flux Phase Lag <u>vs</u> Source Frequency for Two Cadmium Foils in Graphite, at $z = 2, 8, 8.89, 15$, and 30 cm, with Six Spatial Modes	75
11. Age-Diffusion Flux Amplitude <u>vs</u> Distance Along the Z Axis for Two Uranium Foils in D_2O , at 200 cps, with One and Six Spatial Modes	76
12. Components of Age-Diffusion Flux Amplitude <u>vs</u> Distance Along the Z Axis for Two Uranium Foils in D_2O , at 200 cps, with Six Spatial Modes	78
13. Regions of Complex Plane Requiring Different Techniques for Calculating the Error Function	97

Abstract of Dissertation Presented to the Graduate Council
in Partial Fulfillment of the Requirements for the
Degree of Doctor of Philosophy

PROPAGATION OF NEUTRON WAVES THROUGH HETEROGENEOUS
MULTIPLYING AND NONMULTIPLYING MEDIA

By

Victor Ralph Cain

August 1965

Chairman: Dr. Rafael B. Perez
Major Department: Nuclear Engineering

Prediction of the behavior of neutron waves in heterogeneous media is performed using one-group diffusion theory and age-diffusion theory. The one-group theory is used in two different, finite geometries which allow reduction to a one-dimensional problem and to a two-dimensional problem. These cases result in diffusion kernels, or Green's functions, for the two finite configurations.

The theory is then extended to include Fermi-age, or continuous slowing-down, theory for higher energy neutrons. The approach is similar to the Feinberg-Galanin heterogeneous reactor theory except that it is applied to a finite geometry and includes time dependence. A finite diffusion kernel is obtained which is similar to the results of the simpler calculations. In addition, a finite-medium, Fermi-age kernel results which describes the behavior of the slowing-down neutrons in the finite geometry.

Both the one-group and the age-diffusion developments are used to calculate numerically sample configurations which are suitable for experimental verification. These include rectangular assemblies of graphite and heavy water which have poison or fuel rods inserted.

In order to demonstrate better the improvements of this work over the Feinberg-Galanin theory, an extension to critical assemblies is made. This offers the possibility of doing criticality calculations for physically small assemblies which are not amenable to homogenization techniques.

Using the age-diffusion theory results, it is also shown that data from neutron wave experiments may be processed in such a way as to give experimental measurements of both the diffusion and the slowing-down kernel.

INTRODUCTION

In 1960 a program was initiated at the University of Florida in the field of neutron wave propagation. The initial effort was in the determination of diffusion and thermalization parameters in moderating media. It was shown by Perez and Uhrig (1)¹ that these parameters were related to the damping coefficient and phase shift per unit length of the neutron wave. The work of Hartley (2) and Booth (3) confirmed these predictions, and lately Perez and Booth (4) were able to perform accurate measurements of thermalization parameters in graphite using the neutron wave technique. The above mentioned studies were performed in homogeneous neutron moderating media. Some work has been done by Booth (5), in heterogeneous media, and by Denning et al. (6) in two-region moderating media. Denning et al. were able to show a definite reflected wave from the interface between the two media which interferes with the incident wave.

The goal of the present work is to predict, as accurately as is feasible, the propagation of neutron waves in heterogeneous multiplying and nonmultiplying media. The incentive to perform this work is twofold. From the purely academic viewpoint, the propagation of waves through periodic structures is of sufficient interest in the fields of quantum mechanics, sound theory, solid-state physics, and others that extension of the

¹Underlined numbers in parentheses refer to corresponding numbers in the list of references.

previously mentioned work in heterogeneous media becomes desirable. That neutron wave propagation theory is applicable to these other fields may perhaps seem reasonable by pointing out that the neutron wave propagation we are concerned with here is a macroscopic phenomenon, qualitatively similar to sound wave propagation. One simply replaces gas density with neutron density. Quantitatively, the neutron wave propagation is the more difficult problem since nuclear reactors are highly dispersive and absorptive media in which disturbances of the neutron field are quickly damped.

Secondly, there is a strong incentive from the practical viewpoint of gaining understanding about heterogeneous reactors. Traditionally, homogenization techniques based on the Wigner-Seitz unit-cell theory have been used to design heterogeneous reactors, and it is only recently that theories accounting for the interactions between fuel plates are evolving from the works of Galanin (7), Feinberg (8), and others.

The study of neutron wave propagation through heterogeneous media involves analytical techniques and assumptions similar to the developments used in heterogeneous reactor theory. Hence studies of this type offer the possibilities of experimental tests of the various theories in a way which enlarges the realm of application of purely static experiments. Also, any disturbance of the neutron field in a heterogeneous reactor can be analyzed as a superposition of neutron waves, thus yielding information on possible short-range instabilities for a particular reactor design.

Theoretical studies in this field are quite complicated because of the interplay of the effects of the spatial heterogeneities produced by the fuel plates and the energy distribution of the neutron population. Before

meaningful but costly experiments can be performed, the theoretical foundations have to be developed, which is the goal set forth in this dissertation.

At first sight, the obvious approach to the theoretical work is simply to modify the Feinberg-Galatin theory to include time dependence so that it can be applied to subcritical assemblies. In practice, this is not satisfactory since most reactors are rather large assemblies. Because of this the present heterogeneous reactor theory assumes that the moderating medium in which the fuel is embedded is infinite spatially. Practical experimental assemblies for neutron wave propagation experiments, however, tend to be quite small in comparison. Consequently, it was necessary to start from the basic equations including the finiteness of the feasible experimental assemblies.

CHAPTER I

USE OF A ONE-GROUP ONE-DIMENSIONAL GREEN'S FUNCTION IN HETEROGENEOUS MEDIA¹

The problem to be considered is the calculation of the transmission of a thermal neutron wave, according to one-group diffusion theory, in a simple heterogeneous geometry. The geometry chosen is such that it permits a practical experimental setup and also results in an analytical form reducible virtually to a one-dimensional problem.

Figure 1 shows the geometry of the problem. The semi-infinite parallelepiped of moderating material extends from $x = -a$ to $x = a$, $y = -b$ to $y = b$, and $z = 0$ to $z = \infty$. The transverse dimensions a and b are assumed to include the diffusion theory extrapolation distance. The perturbation in the medium is taken to be in the form of very thin sheets, the k th sheet extending from $x = -x_0$ to $x = x_0$ and $y = -b$ to $y = b$ and of thickness h , centered around $z = z_k$. The system is driven by a sinusoidally modulated source of thermal neutrons placed at the face $z = 0$.

The time-dependent, one-group diffusion equation describing this system is

$$\frac{1}{v} \frac{\partial \phi(\underline{r}, t)}{\partial t} = \left\{ D\nabla^2 - [\Sigma_a + \delta\Sigma_a(\underline{r})] \right\} \phi(\underline{r}, t) , \quad (1.1)$$

¹The solution obtained in this chapter is an extension of work originally performed by R. S. Booth.

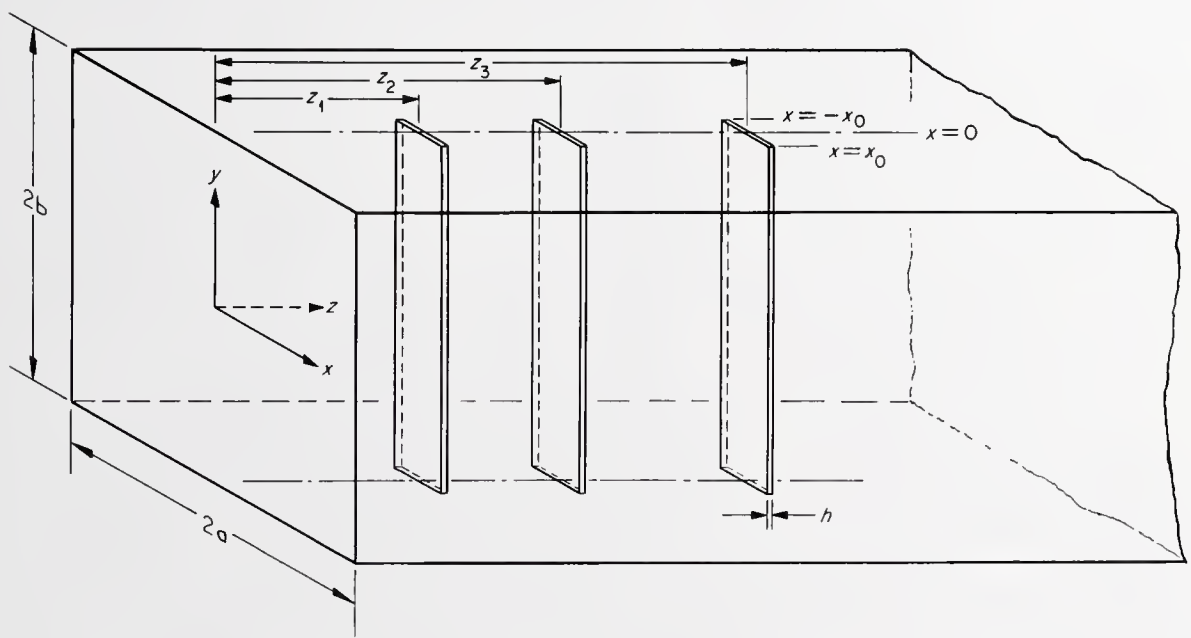


Fig. 1. Geometry for the One-Group, One-Dimension Green's Function Calculation.

where

v = the neutron speed,

$\phi(\underline{r}, t)$ = the spatial and time-dependent neutron flux,

\underline{r} = a position vector,

t = time,

D = the diffusion coefficient (units of length),

∇^2 = the Laplacian operator,

Σ_a = the macroscopic cross section of the moderating media,

$\delta\Sigma_a$ = the space-dependent macroscopic cross section of the absorbing sheets.

The space-dependent perturbation may be written as

$$\delta\Sigma_a(\underline{r}) = \sum_{k=1}^M \delta\Sigma_{a,k} \left[u(x + x_0) - u(x - x_0) \right] \\ \left[u\left(z - z_k + \frac{h}{2}\right) - u\left(z - z_k - \frac{h}{2}\right) \right], \quad (1.2)$$

where $\delta\Sigma_{a,k}$ = the macroscopic cross section of the k th foil, $u(y)$ = the unit step function, and M = the total number of foils. If h is taken to be sufficiently small, the first two terms of the Taylor's series expansion for the unit step function in z may be used in Eq. (1.2), reducing it to

$$\delta\Sigma_a(\underline{r}) = h \left[u(x + x_0) - u(x - x_0) \right] \sum_{k=1}^M \delta\Sigma_{a,k} \delta(z - z_k), \quad (1.3)$$

where $\delta(y)$ is the Dirac delta function.

It should be noted that if the sheets contain fissionable material, $\delta\Sigma_{a,k}$ is replaced by $\delta\Sigma_{a,k} - v\delta\Sigma_{f,k}$, where v is the neutron multiplicity and $\delta\Sigma_{f,k}$ is the macroscopic fission cross section of the k th foil.

The sinusoidally modulated neutron source is assumed to be isotropic with a Maxwellian energy distribution and can be represented by

$$S(\underline{r}, t) = S_0 + \operatorname{Re} \left[S(\underline{r}) \Big|_{z=0} e^{i\omega t} \right] , \quad (1.4)$$

where $i = \sqrt{-1}$, ω is the angular frequency of the modulation and S_0 is the steady component of the source present at $z = 0$. If the neutron flux is assumed to be separable in space and time, the oscillating part of the flux can be represented as (1)

$$\phi(\underline{r}, t) = \operatorname{Re} \left[\phi(\underline{r}) e^{i\omega t} \right] . \quad (1.5)$$

Equation (1.5) may be introduced into Eq. (1.1), resulting in

$$\left[\nabla^2 - \frac{\Sigma_a + \delta\Sigma_a(\underline{r})}{D} \right] \phi(\underline{r}) = \frac{i\omega}{vD} \phi(\underline{r}) , \quad (1.6)$$

or, in slightly different notation,

$$\left[\nabla^2 - \frac{\alpha_0 + i\omega}{D_0} \right] \phi(\underline{r}) = \delta L(x, z) \phi(\underline{r}) , \quad (1.7)$$

where

$$\alpha_0 \equiv v\Sigma_a , \quad (1.8)$$

$$D_0 \equiv vD , \quad (1.9)$$

$$\delta L(x, z) \equiv \delta\Sigma_a(\underline{r})/D . \quad (1.10)$$

The boundary conditions will be taken to be

$$\phi(\underline{r}) \Big|_{x=\pm a} = \phi(\underline{r}) \Big|_{y=\pm b} = \lim_{z \rightarrow \infty} \phi(\underline{r}) = 0 . \quad (1.11)$$

In addition, at the source plane,

$$-D \frac{\partial \phi(\underline{r}, t)}{\partial z} \Big|_{z=0} = \frac{1}{2} \operatorname{Re} \left[S(\underline{r}) \Big|_{z=0} e^{i\omega t} \right] . \quad (1.12)$$

Using Eq. (1.5), this reduces to

$$-D \frac{\partial \phi(\underline{r})}{\partial z} \Big|_{z=0} = \frac{1}{2} S(\underline{r}) \Big|_{z=0} . \quad (1.13)$$

The spatial flux, $\phi(\underline{r})$, may be represented by an expansion in the complete set of transverse eigenfunctions defined by

$$(\nabla^2 + B_{\ell m}^2) \phi_{\ell m}(x, y) = 0 \quad (1.14)$$

and by the boundary conditions at $x = \pm a$ and $y = \pm b$ plus the conditions of symmetry around $x = 0$ and $y = 0$. Normalized, these eigenfunctions and their related eigenvalues are

$$\phi_{\ell m}(x, y) = \frac{1}{\sqrt{ab}} \cos \frac{(2\ell - 1)\pi x}{2a} \cos \frac{(2m - 1)\pi y}{2b} , \quad (1.15)$$

and

$$B_{\ell m}^2 = \left[\frac{(2\ell - 1)\pi}{2a} \right]^2 + \left[\frac{(2m - 1)\pi}{2b} \right]^2 , \quad (1.16)$$

where ℓ and m may take on all integral values.

The expansion of $\phi(\underline{r})$ is given by

$$\phi(\underline{r}) = \sum_{\ell, m} \phi_{\ell m}(z) \phi_{\ell m}(x, y) . \quad (1.17)$$

Substituting Eq. (1.17) into Eq. (1.7) gives

$$\left[\nabla^2 - \frac{\alpha_0 + i\omega}{D_0} \right] \sum_{\ell, m} \phi_{\ell m}(x, y) \phi_{\ell m}(z) = \delta L(x, z) \sum_{\ell, m} \phi_{\ell m}(x, y) \phi_{\ell m}(z) . \quad (1.18)$$

Operating on Eq. (1.18) with $\int_{-a}^a dx \int_{-b}^b dy \phi_{pq}(x, y)$ results in

$$\left[\frac{d^2}{dz^2} - \rho_{pq}^2 \right] \phi_{pq}(z) = \sum_{\ell, m} \delta L_{pq\ell m}(z) \phi_{\ell m}(z) , \quad (1.19)$$

where

$$\rho_{pq}^2 \equiv B_{\perp pq}^2 + \frac{\alpha_0 + i\omega}{D_0} , \quad (1.20)$$

and

$$\delta L_{pq\ell m}(z) \equiv \int_{-a}^a dx \int_{-b}^b dy \phi_{pq}(x, y) \delta L(x, z) \phi_{\ell m}(x, y) . \quad (1.21)$$

Before continuing further with Eq. (1.19), note that the two boundary conditions in z have yet to be applied. In order to make use of the source boundary condition, $S(\underline{r})$ must be expanded in the same transverse eigenfunctions. That is,

$$S(\underline{r}) \Big|_{z=0} = \sum_{\ell, m} S_{\ell m} \phi_{\ell m}(x, y) , \quad (1.22)$$

where

$$S_{\ell m} = \int_{-a}^a dx \int_{-b}^b dy S(\underline{r}) \Big|_{z=0} \phi_{\ell m}(x, y) . \quad (1.23)$$

It should be pointed out that this expansion, as well as the flux expansion, assumes symmetry around the x and y axes. If one uses a source containing asymmetric components, $\phi_{\ell m}(x, y)$ must also include sine terms. Inserting the expansions, Eqs. (1.17) and (1.22), into the source boundary condition, Eq. (1.13), gives

$$-D \frac{d\phi_{\ell m}(z)}{dz} \Big|_{z=0} = \frac{S_{\ell m}}{2} . \quad (1.24)$$

The boundary condition at $z = \infty$ becomes

$$\lim_{z \rightarrow \infty} \phi_{\ell m}(z) = 0 . \quad (1.25)$$

Now returning to the reduction of Eq. (1.19), substitute Eqs. (1.3) and (1.10) into Eq. (1.21). The y integration may be performed immediately, yielding δ_{qm} , the Kronecker delta. Also performing the x integration gives the result

$$\delta L_{pq\ell m}(z) = \frac{h}{D} \delta_{qm} \delta F_{p\ell} \sum_{k=1}^M \delta \Sigma_{a,k} \delta(z - z_k) , \quad (1.26)$$

where $\delta F_{p\ell}$ is given by

Now define the Green's function $G_{pq}(z, \xi)$, satisfying

$$\left[\frac{\partial^2}{\partial \xi^2} - \rho_{pq}^2 \right] G_{pq}(z, \xi) = - \frac{\delta(z - \xi)}{D} \quad (1.32)$$

and the homogeneous forms of the boundary conditions satisfied by $\phi_{pq}(z)$.

Multiply Eq. (1.30) by $G_{pq}(z, \xi)$ and Eq. (1.32) by $\phi_{pq}(\xi)$. Subtract the

two results and operate with $\int_0^\infty d\xi$ to obtain

$$\int_0^\infty d\xi \left\{ G(z, \xi) \frac{d^2 \phi(\xi)}{d\xi^2} - \phi(\xi) \frac{\partial^2 G(z, \xi)}{\partial \xi^2} \right\} - \int_0^\infty d\xi F(\xi) G(z, \xi) = \frac{\phi(z)}{D} . \quad (1.33)$$

The subscripts have been dropped temporarily for economy of notation.

Integrating the first integral by parts results in

$$\begin{aligned} \phi(z) &= D \left\{ G(z, \xi) \frac{d\phi(\xi)}{d\xi} - \phi(\xi) \frac{\partial G(z, \xi)}{\partial \xi} \right\} \Big|_0^\infty \\ &- D \int_0^\infty d\xi \frac{\partial G(z, \xi)}{\partial \xi} \frac{d\phi(\xi)}{d\xi} + D \int_0^\infty d\xi \frac{d\phi(\xi)}{d\xi} \frac{\partial G(z, \xi)}{\partial \xi} \\ &- D \int_0^\infty d\xi F(\xi) G(z, \xi) . \end{aligned} \quad (1.34)$$

The first two integrals cancel, both ϕ and G go to zero as $\xi \rightarrow \infty$, and the gradient of G is zero at $\xi = 0$. Therefore, the desired integral equation is

$$\phi(z) = - D G(z, \xi) \frac{d\phi}{d\xi} \Big|_{\xi=0} - D \int_0^\infty d\xi F(\xi) G(z, \xi) . \quad (1.35)$$

$$\delta F_{pq} = \frac{\sin \frac{(\ell - p)\pi x_0}{a}}{(\ell - p)\pi} + \frac{\sin \frac{(\ell + p - 1)\pi x_0}{a}}{(\ell + p - 1)\pi}, \quad \ell \neq p$$

$$= \frac{x_0}{a} + \frac{\sin \frac{(2\ell - 1)\pi x_0}{a}}{(2\ell - 1)\pi}, \quad \ell = p.$$
(1.27)

In order to simplify Eq. (1.27) further, let us assume that x_0 is sufficiently less than a that the first term of the Maclaurin's series may be used for the sine terms. Equation (1.27) then becomes

$$\delta F_{pq} \approx \frac{2x_0}{a}, \quad \text{for all } \ell \text{ and } p.$$
(1.28)

Now inserting Eq. (1.26) and Eq. (1.28) into Eq. (1.19) gives

$$\left[\frac{d^2}{dz^2} - \rho_{pq}^2 \right] \phi_{pq}(z) = \frac{2hx_0}{a} \sum_{\ell} \sum_{k=1}^M \delta \Sigma_{a,k} \delta(z - z_k) \phi_{\ell q}(z). \quad (1.29)$$

It may be noted from the above equation that the one-dimensional problem turns out to be not really one dimensional, in the sense that coupling remains between the spatial harmonics associated with the x direction.

In order to solve Eq. (1.29), it is convenient to convert it into an integral equation. Substitute ξ for z and rewrite as

$$\left[\frac{d^2}{d\xi^2} - \rho_{pq}^2 \right] \phi_{pq}(\xi) = F_{pq}(\xi), \quad (1.30)$$

where

$$F_{pq}(\xi) = \frac{2hx_0}{Da} \sum_{\ell} \sum_{k=1}^M \delta \Sigma_{a,k} \delta(\xi - z_k) \phi_{\ell q}(\xi). \quad (1.31)$$

The problem now is to determine the Green's function defined by Eq. (1.32). The solution to the homogeneous form of Eq. (1.32) is

$$G(\xi, z) = Ae^{-\rho z} + Ce^{\rho z}, \quad (1.36)$$

where ξ and z have been switched. The particular integral of Eq. (1.32) may be found by the technique of the variation of parameters. Let the constants in Eq. (1.36) depend on z (they also depend on ξ , of course, but this may be ignored at this point):

$$G(\xi, z) = A(z)e^{-\rho z} + C(z)e^{\rho z}. \quad (1.37)$$

Differentiation of Eq. (1.37) gives

$$\frac{\partial G(\xi, z)}{\partial z} = -\rho A(z)e^{-\rho z} + \rho C(z)e^{\rho z} + \frac{dA}{dz}e^{-\rho z} + \frac{dC}{dz}e^{\rho z}. \quad (1.38)$$

Choose A and C such that

$$\frac{dA}{dz}e^{-\rho z} + \frac{dC}{dz}e^{\rho z} = 0; \quad (1.39)$$

Then differentiate again:

$$\frac{\partial^2 G(\xi, z)}{\partial z^2} = \rho^2 A(z)e^{-\rho z} + \rho^2 C(z)e^{\rho z} - \rho \frac{dA}{dz}e^{-\rho z} + \rho \frac{dC}{dz}e^{\rho z}. \quad (1.40)$$

Inserting Eqs. (1.40) and (1.37) into the original differential equation for the Green's function results in

$$\begin{aligned} A \left[\rho^2 e^{-\rho z} - \rho^2 e^{-\rho z} \right] + C \left[\rho^2 e^{\rho z} - \rho^2 e^{\rho z} \right] \\ + \frac{dA}{dz} \left[-\rho e^{-\rho z} \right] + \frac{dC}{dz} \left[\rho e^{\rho z} \right] = -\frac{\delta(z - \xi)}{D}, \end{aligned} \quad (1.41)$$

or

$$-\rho e^{-\rho z} \frac{dA}{dz} + \rho e^{\rho z} \frac{dC}{dz} = -\frac{\delta(z - \xi)}{D} . \quad (1.42)$$

Equations (1.39) and (1.42) are two equations in dA/dz and dC/dz which may be solved simultaneously to give

$$\frac{dA}{dz} = \frac{\delta(z - \xi)}{2\rho D} e^{\rho z} \quad (1.43)$$

and

$$\frac{dC}{dz} = -\frac{\delta(z - \xi)}{2\rho D} e^{-\rho z} . \quad (1.44)$$

Integrating Eqs. (1.43) and (1.44) gives

$$A = e^{\rho \xi} / 2\rho D + B \quad (1.45)$$

and

$$C = -e^{-\rho \xi} / 2\rho D + E , \quad (1.46)$$

where B and E are constants to be determined from the boundary conditions.

Using Eqs. (1.45) and (1.46) in Eq. (1.36) gives

$$G(\xi, z) = Be^{-\rho z} + Ee^{\rho z} + \frac{e^{\rho(\xi-z)}}{2\rho D} - \frac{e^{-\rho(\xi-z)}}{2\rho D} \quad (1.47)$$

or

$$G(\xi, z) = Be^{-\rho z} + Ee^{\rho z} + \frac{\sinh \rho(\xi - z)}{\rho D} . \quad (1.48)$$

The one-dimensional Green's function has a discontinuity in slope at the

source point, $z = \xi$. Actually, this does not need to be known beforehand, since straightforward application of the only two boundary conditions now available leads to the solution $G \equiv 0$. Then, in order to obtain a solution, before applying the boundary conditions, Eq. (1.48) must be divided into two parts, one which will apply for $z < \xi$ and the other for $z > \xi$. Now, two more boundary conditions are needed, which may be found by integrating Eq. (1.32) over a small region including the source point:

$$\int_{\xi-\epsilon}^{\xi+\epsilon} dz \left[\frac{d^2}{dz^2} - \rho^2 \right] G(\xi, z) = - \int_{\xi-\epsilon}^{\xi+\epsilon} dz \frac{\delta(z - \xi)}{D} . \quad (1.49)$$

Assuming that the second derivative is more singular than the function itself, one obtains, in the limit of small ϵ ,

$$\left. \frac{\partial G(\xi, z)}{\partial z} \right|_{\xi+\epsilon} - \left. \frac{\partial G(\xi, z)}{\partial z} \right|_{\xi-\epsilon} = - \frac{1}{D} . \quad (1.50)$$

Therefore the two boundary conditions are continuity of G at $z = \xi$ and Eq. (1.50), which gives the magnitude of the discontinuity in the first derivative.

The two parts of the solution will be denoted as

$$G^L(\xi, z) = B^L e^{-\rho z} + E^L e^{\rho z} + \frac{\sinh \rho(\xi - z)}{\rho D} , \quad z < \xi , \quad (1.51)$$

and

$$G^R(\xi, z) = B^R e^{-\rho z} + E^R e^{\rho z} + \frac{\sinh \rho(\xi - z)}{\rho D} , \quad z > \xi . \quad (1.52)$$

The $z = 0$ boundary condition is

$$\left. \frac{dG^L(\xi, z)}{dz} \right|_{z=0} = -\rho B^L + \rho E^L - \frac{\cosh \rho \xi}{D} = 0 \quad . \quad (1.53)$$

At large z , the boundary condition is

$$\lim_{z \rightarrow \infty} G^R(\xi, z) = \lim_{z \rightarrow \infty} \left[E^R e^{\rho z} - \frac{e^{-\rho \xi} e^{\rho z}}{2\rho D} \right] = 0 \quad . \quad (1.54)$$

Equation (1.54) immediately determines E^R :

$$E^R = \frac{e^{-\rho \xi}}{2\rho D} \quad . \quad (1.55)$$

The continuity condition, at $z = \xi$, leads to

$$B^L e^{-\rho \xi} + E^L e^{\rho \xi} = B^R e^{-\rho \xi} + E^R e^{\rho \xi} \quad . \quad (1.56)$$

Equation (1.50) becomes

$$-\rho B^R e^{-\rho \xi} + \rho E^R e^{\rho \xi} - \frac{1}{D} + \rho B^L e^{-\rho \xi} - \rho E^L e^{\rho \xi} + \frac{1}{D} = -\frac{1}{D} \quad . \quad (1.57)$$

Using Eq. (1.55), Eqs. (1.53), (1.56), and (1.57) may be put in matrix form as

$$\begin{pmatrix} -\rho & \rho & 0 \\ e^{-\rho \xi} & e^{\rho \xi} & -e^{-\rho \xi} \\ -\rho e^{-\rho \xi} & \rho e^{\rho \xi} & \rho e^{-\rho \xi} \end{pmatrix} \begin{pmatrix} B^L \\ E^L \\ B^R \end{pmatrix} = \begin{pmatrix} \frac{\cosh \rho \xi}{D} \\ \frac{1}{2\rho D} \\ \frac{3}{2D} \end{pmatrix} \quad . \quad (1.58)$$

The three solutions to Eq. (1.58) are

$$B^L = - \frac{\sinh \rho\xi}{\rho D} , \quad (1.59)$$

$$E^L = \frac{e^{-\rho\xi}}{\rho D} , \quad (1.60)$$

$$B^R = \frac{e^{-\rho\xi}}{2\rho D} . \quad (1.61)$$

Upon substituting Eqs. (1.55), (1.59), (1.60), and (1.61) into Eqs. (1.51) and (1.52) and rearranging, one obtains

$$G^L(\xi, z) = \frac{e^{-\rho\xi}}{\rho D} \cosh \rho z , \quad z < \xi , \quad (1.62)$$

and

$$G^R(\xi, z) = \frac{e^{-\rho z}}{\rho D} \cosh \rho\xi , \quad z > \xi . \quad (1.63)$$

It may be noticed that Eqs. (1.62) and (1.63) define a function which is symmetric with respect to interchange of the coordinates of the source and observer locations (z and ξ), thus satisfying one of the necessary criteria for a Green's function (9). Equation (1.63) may now be substituted into Eq. (1.55), giving

$$\begin{aligned} \phi(z) = & - D \left. \frac{e^{-\rho z}}{\rho D} \frac{d\phi}{d\xi} \right|_{\xi=0} - D \int_0^z \frac{e^{-\rho z}}{\rho D} \cosh \rho\xi F(\xi) d\xi \\ & - D \int_z^\infty \frac{e^{-\rho\xi}}{\rho D} \cosh \rho z F(\xi) d\xi . \end{aligned} \quad (1.64)$$

Reinserting subscripts and using Eq. (1.24), one obtains

$$\begin{aligned} \phi_{pq}(z) = & \frac{s_{pq} e^{-\rho_{pq} z}}{2\rho_{pq} D} - \frac{e^{-\rho_{pq} z}}{\rho_{pq}} \int_0^z d\xi \cosh \rho_{pq} \xi F_{pq}(\xi) \\ & - \frac{\cosh \rho_{pq} z}{\rho_{pq}} \int_z^\infty d\xi e^{-\rho_{pq} \xi} F_{pq}(\xi) . \end{aligned} \quad (1.65)$$

Since $F_{pq}(\xi)$ contains δ functions in ξ , Eq. (1.31) may be inserted into Eq. (1.65) and the integrals in ξ performed, leading to

$$\begin{aligned} \phi_{pq}(z) = & \frac{s_{pq} e^{-\rho_{pq} z}}{2\rho_{pq} D} - \frac{2hx_o}{\rho_{pq} Da} \left\{ e^{-\rho_{pq} z} \sum_{\ell} \sum_{k=1}^{M'} \delta \Sigma_{a,k} \cosh \rho_{pq} z_k \phi_{\ell q}(z_k) \right. \\ & \left. + \cosh \rho_{pq} z \sum_{\ell} \sum_{k=M'+1}^M \delta \Sigma_{a,k} e^{-\rho_{pq} z_k} \phi_{\ell q}(z_k) \right\} , \end{aligned} \quad (1.66)$$

where M' is determined by $z_{M'} \leq z \leq z_{M'+1}$. If z equals one of the z_k 's, it can be taken to be either $z_{M'}$ or $z_{M'+1}$ since the Green's function is continuous at the source point.

In order to obtain a solution to this system, the original expansion of $\phi(\underline{r})$, Eq. (1.17), must be truncated. Assume that the desired approximation is

$$\phi(\underline{r}) \approx \sum_{\ell=1}^L \sum_{q=1}^Q \phi_{\ell q}(z) \phi_{\ell q}(x, y) . \quad (1.67)$$

For each value of q , a set of LM simultaneous equations may be obtained from Eq. (1.66) by writing it for each of the L modes and for $z = z_1, z_2, \dots, z_M$. This set determines each of the LM values of $\phi_{\ell q}(z_k)$.

Writing these values as a vector, where the superscript T indicates the transpose,

$$\Phi_q^T = \left[\phi_{1q}(z_1), \phi_{1q}(z_2), \dots \phi_{1q}(z_M), \phi_{2q}(z_1), \dots \phi_{Lq}(z_M) \right] , \quad (1.68)$$

the set of equations may be put into matrix form. That is,

$$\left[A_q \right] \Phi_q + \left[I \right] \Phi_q = B_q , \quad (1.69)$$

where $[I]$ is the identity matrix, the vector B_q contains the constant (source) terms, and the matrix $[A_q]$ contains the Green's functions. B_q may be written as

$$B_q^T = \left[\alpha_{1q} e^{-\rho_{1q} z_1}, \alpha_{1q} e^{-\rho_{1q} z_2}, \dots, \alpha_{Lq} e^{-\rho_{Lq} z_M} \right] , \quad (1.70)$$

where

$$\alpha_{\ell q} \equiv \frac{s_{\ell q}}{2 \rho_{\ell q} D} . \quad (1.71)$$

The $[A_q]$ matrix may be partitioned into L^2 submatrices which are each M by M. The n,p element of the I,J submatrix is given by

$$(A_{I,J})_{n,p} = \beta_{Iq}(z_p) \cosh \rho_{Iq} z_p e^{-\rho_{Iq} z_n} , \quad n > p , \quad (1.72)$$

or

$$(A_{I,J})_{n,p} = \beta_{Iq}(z_p) \cosh \rho_{Iq} z_n e^{-\rho_{Iq} z_p} , \quad n < p , \quad (1.73)$$

where

$$\beta_{Iq}(z_p) \equiv \frac{2hx_o}{\rho_{Iq}} \frac{\delta\Sigma_{a,p}}{Da} . \quad (1.74)$$

Solving Eq. (1.69) Q times by inverting the matrix $[A_q] + [I]$ gives the Φ_q 's:

$$\Phi_q = \left[[A_q] + [I] \right]^{-1} B_q , \quad (1.75)$$

which may be inserted into the summations in Eq. (1.66). The results of Eq. (1.66) are then inserted into Eq. (1.67) to give the desired approximation to the spatial flux $\phi(\underline{r})$.

CHAPTER II

USE OF A ONE-GROUP TWO-DIMENSIONAL GREEN'S FUNCTION IN HETEROGENEOUS MEDIA

The problem of the previous chapter will now be extended to two dimensions by allowing the perturbations to be placed anywhere in the x - z plane contained in the moderating material. Equation (1.1) will still apply, but now $\delta\Sigma_a(\underline{r})$ will be taken to be a general function of x and z . Equation (1.7), with its boundary conditions given in Eqs. (1.11) and (1.13), will be taken as the starting point, leaving $\delta L(x, z)$ general.

In this case the spatial flux $\phi(\underline{r})$ will be expanded in the single set of transverse eigenfunctions, defined by

$$\left[\frac{d^2}{dy^2} + B_m^2 \right] \phi_m(y) = 0 \quad (2.1)$$

and the boundary conditions $\phi_m(+b) = 0$ and $\phi_m(y) = \phi_m(-y)$. The eigenfunctions are

$$\phi_m(y) = \frac{1}{\sqrt{b}} \cos \frac{(2m - 1)\pi y}{2b} , \quad (2.2)$$

and the eigenvalues are

$$B_m^2 = \left[\frac{(2m - 1)\pi}{2b} \right]^2 , \quad (2.3)$$

where $m = 1, 2, 3, \dots$. Using the following expansions of the flux and the source,

$$\phi(\underline{r}) = \sum_m \phi_m(x, z) \phi_m(y) \quad (2.4)$$

and

$$S(\underline{r}) = \sum_m S_m(x) \phi_m(y) , \quad (2.5)$$

in Eqs. (1.7) and (1.13) gives

$$\left[\nabla^2 - \frac{\alpha_o + i\omega}{D_o} \right] \sum_m \phi_m(x, z) \phi_m(y) = \delta L(x, z) \sum_m \phi_m(x, z) \phi_m(y) , \quad (2.6)$$

and

$$-D \frac{\partial}{\partial z} \sum_m \phi_m(x, z) \phi_m(y) \Big|_{z=0} = \frac{1}{2} \sum_m S_m(x) \phi_m(y) . \quad (2.7)$$

Operating with $\int_{-b}^b dy \phi_n(y)$ gives

$$\left[\frac{\partial^2}{\partial x^2} + \frac{\partial^2}{\partial z^2} - \rho_n^2 \right] \phi_n(x, z) = \delta L(x, z) \phi_n(x, z) , \quad (2.8)$$

where

$$\rho_n^2 \equiv B_n^2 + \frac{\alpha_o + i\omega}{D_o} \quad (2.9)$$

and the corresponding boundary condition

$$-D \frac{\partial \phi_n(x, z)}{\partial z} \Big|_{z=0} = \frac{1}{2} S_n(x) . \quad (2.10)$$

The remaining boundary conditions given in Eq. (1.11) still apply.

It is evident that this system may be treated similarly to the previous problem if a two-dimensional Green's function can be found which is the solution of

$$\left[\frac{\partial^2}{\partial x^2} + \frac{\partial^2}{\partial z^2} - \rho_n^2 \right] G_n(x, z; x_o, z_o) = -\delta(x - x_o) \delta(z - z_o) , \quad (2.11)$$

with boundary conditions

$$G_n(\pm a, z; x_o, z_o) = \left. \frac{\partial G_n}{\partial z} \right|_{z=0} = \lim_{z \rightarrow \infty} G_n = 0 . \quad (2.12)$$

This Green's function may be found by expanding in the eigenfunctions of

$$\left[\frac{d^2}{dx^2} + \underline{k}^2 \right] \psi_{\underline{k}}(x) = 0; \quad \psi_{\underline{k}}(\pm a) = 0 . \quad (2.13)$$

These are

$$\psi_{\ell}(x) = A_{\ell} \cos \frac{(2\ell - 1)\pi x}{2a} + B_{\ell} \sin \frac{\ell\pi x}{a} . \quad (2.14)$$

Note that \underline{k} assumes two different values for the two different eigenfunctions, the sine and the cosine. The expansion of $G_n(x, z; x_o, z_o)$ is

$$G_n(x, z; x_o, z_o) = \sum_{\ell} C_{\ell}(z, z_o) \left[A_{\ell}(x_o) \cos \frac{(2\ell - 1)\pi x}{2a} + B_{\ell}(x_o) \sin \frac{\ell\pi x}{a} \right] . \quad (2.15)$$

Inserting Eq. (2.15) into Eq. (2.11) gives, with arguments dropped for convenience,

$$\begin{aligned}
& \sum_{\ell} C_{\ell} \left[-A_{\ell} \left\{ \frac{(2\ell - 1)\pi}{2a} \right\}^2 \cos \frac{(2\ell - 1)\pi x}{2a} - B_{\ell} \left\{ \frac{\ell\pi}{a} \right\}^2 \sin \frac{\ell\pi x}{a} \right] \\
& + \sum_{\ell} \frac{\partial^2 C_{\ell}}{\partial z^2} \left[A_{\ell} \cos \frac{(2\ell - 1)\pi x}{2a} + B_{\ell} \sin \frac{\ell\pi x}{a} \right] - \rho_n^2 \sum_{\ell} C_{\ell} \\
& \left[A_{\ell} \cos \frac{(2\ell - 1)\pi x}{2a} + B_{\ell} \sin \frac{\ell\pi x}{a} \right] = -\delta(x - x_o) \delta(z - z_o) . \quad (2.16)
\end{aligned}$$

Operating on Eq. (2.16), in turn, with $\int_{-a}^a \cos \frac{(2j - 1)\pi x}{2a} dx$ and with

$$\int_{-a}^a \sin \frac{j\pi x}{a} dx$$
 gives

$$- C_j A_j \left\{ \frac{(2j - 1)\pi}{2a} \right\}^2 a + \frac{\partial^2 C_j}{\partial z^2} A_j a - \rho_n^2 C_j A_j a = -\delta(z - z_o) \cos \frac{(2j - 1)\pi x_o}{2a} , \quad (2.17)$$

and

$$- C_j B_j \left\{ \frac{j\pi}{a} \right\}^2 a + \frac{\partial^2 C_j}{\partial z^2} B_j a - \rho_n^2 C_j B_j a = -\delta(z - z_o) \sin \frac{j\pi x_o}{a} . \quad (2.18)$$

These two expressions may be rewritten so as to have the left-hand sides functions of z and z_o only and the right-hand sides functions of x_o only.

They become

$$\frac{\frac{\partial^2 C_j}{\partial z^2} - \left[\rho_n^2 + \left\{ \frac{(2j - 1)\pi}{2a} \right\}^2 \right] C_j}{-\delta(z - z_o)} = \frac{\cos \frac{(2j - 1)\pi x_o}{2a}}{a A_j} , \quad (2.19)$$

and

$$\frac{\frac{\partial^2 C_j}{\partial z^2} - \left[\rho_n^2 + \left(\frac{j\pi}{a} \right)^2 \right] C_j}{-\delta(z - z_0)} = \frac{\sin \frac{j\pi x_0}{a}}{a B_j} . \quad (2.20)$$

Obviously the C_j 's in the above two equations are not the same; so the C_j will be replaced by A'_j in Eq. (2.19) and by B'_j in Eq. (2.20). Notice also that both sides of Eqs. (2.19) and (2.20) are equal to constants and no loss in generality occurs if this constant is taken to be unity in each equation. With this step, A_j and B_j may be obtained immediately:

$$A_j(x_0) = \frac{1}{a} \cos \frac{(2j - 1)\pi x_0}{2a} \quad (2.21)$$

and

$$B_j(x_0) = \frac{1}{a} \sin \frac{j\pi x_0}{a} , \quad (2.22)$$

and with the definitions

$$\mu^2 \equiv \rho_n^2 + \left\{ \frac{(2j - 1)\pi}{2a} \right\}^2 \quad (2.23)$$

and

$$\eta^2 \equiv \rho_n^2 + \left\{ \frac{j\pi}{a} \right\}^2 \quad (2.24)$$

the two equations for A'_j and B'_j are

$$\left[\frac{\partial^2}{\partial z^2} - \mu^2 \right] A'_j(z, z_0) = -\delta(z - z_0) \quad (2.25)$$

and

$$\left[\frac{\partial^2}{\partial z^2} - \eta^2 \right] B_j'(z, z_o) = -\delta(z - z_o) . \quad (2.26)$$

The related boundary conditions are

$$\left. \frac{\partial A_j'}{\partial z} \right|_{z=0} = \left. \frac{\partial B_j'}{\partial z} \right|_{z=0} = \lim_{z \rightarrow \infty} A_j' = \lim_{z \rightarrow \infty} B_j' = 0 , \quad (2.27)$$

plus the function continuities and first-derivative discontinuities at $z = z_o$. These functions are virtually identical to the one-dimensional Green's function developed in Chapter I and can therefore be immediately written down, being

$$A_j'(z, z_o) = \frac{e^{-\mu z_o} \cosh \mu z}{\mu} , \quad z < z_o$$

$$= \frac{e^{-\mu z} \cosh \mu z_o}{\mu} , \quad z > z_o , \quad (2.28)$$

and

$$B_j'(z, z_o) = \frac{e^{-\eta z_o} \cosh \eta z}{\eta} , \quad z < z_o$$

$$= \frac{e^{-\eta z} \cosh \eta z_o}{\eta} , \quad z > z_o . \quad (2.29)$$

Collecting Eqs. (2.21), (2.22), (2.28), and (2.29) into Eq. (2.15), the complete Green's function is

$$G_n(x, z; x_o, z_o) = \sum_{\ell} \left[\frac{e^{-\mu z_o}}{\mu a} \cosh \frac{\mu z}{\mu a} \cos \frac{(2\ell - 1)\pi x_o}{2a} \cos \frac{(2\ell - 1)\pi x}{2a} \right. \\ \left. + \frac{e^{-\eta z_o}}{\eta a} \cosh \frac{\eta z}{\eta a} \sin \frac{\ell \pi x_o}{a} \sin \frac{\ell \pi x}{a} \right], \quad z < z_o \quad (2.30)$$

and

$$G_n(x, z; x_o, z_o) = \sum_{\ell} \left[\frac{e^{-\mu z}}{\mu a} \cosh \frac{\mu z_o}{\mu a} \cos \frac{(2\ell - 1)\pi x_o}{2a} \cos \frac{(2\ell - 1)\pi x}{2a} \right. \\ \left. + \frac{e^{-\eta z}}{\eta a} \cosh \frac{\eta z_o}{\eta a} \sin \frac{\ell \pi x_o}{a} \sin \frac{\ell \pi x}{a} \right], \quad z > z_o \quad (2.31)$$

Similarly to the procedure followed previously, this Green's function may be used to formulate an integral equation for $\phi_n(x, z)$. x_o and z_o are interchanged with x and z in Eqs. (2.8) and (2.11). The difference between $G_n(x_o, z_o; x, z)$ times Eq. (2.8) and $\phi_n(x_o, z_o)$ times (2.11) is taken. The result is operated on with $\int_0^\infty dz_o \int_{-a}^a dx_o$ to give, with arguments and integration limits dropped,

$$\int dz_o \int dx_o G_n \frac{\partial^2 \phi_n}{\partial x_o^2} + \int dz_o \int dx_o G_n \frac{\partial^2 \phi_n}{\partial z_o^2} - \int dz_o \int dx_o \phi_n \frac{\partial^2 G_n}{\partial x_o^2} \\ - \int dz_o \int dx_o \phi_n \frac{\partial^2 G_n}{\partial z_o^2} = \int dz_o \int dx_o G_n \delta L \phi_n + \phi_n(x, z) . \quad (2.32)$$

In the terms containing partials with respect to x , an integration by parts in x may be done, and similarly with the z partials. All remaining surface

integrals on the left-hand side of Eq. (2.32) cancel and most of the line integrals are eliminated by the boundary conditions. The remaining terms give

$$\begin{aligned}\phi_n(x, z) = & - \int_{-a}^a dx_o G_n(x_o, z_o; x, z) \left| \frac{\partial \phi_n(x_o, z_o)}{\partial z_o} \right|_{z_o=0} \\ & - \int_0^\infty dz_o \int_{-a}^a dx_o G_n(x_o, z_o; x, z) \delta L(x_o, z_o) \phi_n(x_o, z_o) .\end{aligned}\quad (2.33)$$

Equations (2.10), (2.30), and (2.31) are to be substituted into Eq. (2.33), along with the desired form of $\delta L(x_o, z_o)$, in order to obtain the integral equation for $\phi_n(x, z)$.

If the form of $\delta L(x, z)$ of Chapter I is used in Eq. (2.33), it is straightforward although rather tedious to show that Eq. (2.33) reduces to Eq. (1.66). To do this, the following expansions must be used:

$$\phi_n(x, z) = \sum_j \phi_{jn}(z) \phi_j(x) \quad (2.34)$$

and

$$s_n(x) = \sum_j s_{jn} \phi_j(x) , \quad (2.35)$$

where

$$\phi_j(x) = \frac{1}{\sqrt{a}} \cos \frac{(2j - 1)\pi x}{2a} . \quad (2.36)$$

These expansions are justified, since if δL is symmetric in x [and it is assumed as before that $S(\underline{r})$ is symmetric around the x and y axes], then ϕ_n will also be symmetric in x . It is then a matter of performing the x_0

and z_0 integrations in Eq. (2.33) and operating with $\int_{-a}^a \frac{1}{\sqrt{a}} \cos \frac{(2p-1)\pi x}{2a} dx$

to obtain Eq. (1.66).

CHAPTER III

USE OF AN AGE-DIFFUSION TWO-DIMENSIONAL GREEN'S FUNCTION IN HETEROGENEOUS MEDIA

The development of this chapter is similar to that of the preceding chapter except that the theory is to be the continuous slowing-down model with a thermal group. The geometry is the same semi-infinite moderating medium, with the perturbations now being small fuel rods which, as before, run the full length of the y axis. This model is similar to the Feinberg-Galanin treatment of heterogeneous reactors (7) and (8), with two major exceptions. In this study time dependence is included and the finiteness of the medium is taken into account. This will result in a finite medium Fermi-age kernel, or Green's function, as well as the corresponding diffusion kernel obtained in the previous developments of this work.

For lethargies below thermal, the applicable equation is

$$- D(u) \nabla^2 \phi(\underline{r}, u, t) + \Sigma_a(u) \phi(\underline{r}, u, t) = - \frac{1}{v(u)} \frac{\partial \phi(\underline{r}, u, t)}{\partial t} + S(\underline{r}, u, t) - \frac{\partial q(\underline{r}, u, t)}{\partial u} , \quad (3.1)$$

where the nomenclature is similar to that previously used except that now all quantities are lethargy-dependent and S and q represent the neutron source and slowing-down density, respectively. It has been assumed that $\Sigma_a(u)$ for $u < u_s$, where u_s is the thermal neutron lethargy, is independent of position. This is valid as long as the fuel rods are small.

The relation between the flux and slowing-down density applicable to an infinite medium will be assumed, that is, that

$$q(\underline{r}, u, t) = \xi \Sigma_t(u) \phi(\underline{r}, u, t) , \quad (3.2)$$

where ξ = the average logarithmic energy decrement, and $\Sigma_t(u)$ = the total macroscopic cross section in the moderating media.

The thermal group is described as before, except for the addition of the source of thermal neutrons from the slowing-down density. This relation is

$$\left[- D_s \nabla^2 + \Sigma_{as} + \frac{1}{v_s} \frac{\partial}{\partial t} \right] \phi_s(\underline{r}, t) = q(\underline{r}, u_s, t) - A(\underline{r}, t) , \quad (3.3)$$

where $A(\underline{r}, t)$ represents the absorption in the fuel rods and the subscript s indicates that the quantity is evaluated at the thermal neutron energy.

In order to define the quantities $S(\underline{r}, u, t)$ and $A(\underline{r}, t)$, it will be assumed that (1) all fission neutrons are born at lethargy $u = 0$, (2) all fuel rods are lines, the k th rod being representable as $\delta(x - x_k) \delta(z - z_k)$, and (3) the driving source is located at $z = 0$, producing only thermal neutrons and is of the form $\text{Re}[S(x, y) \delta(z) e^{i\omega t}]$. As before, since the source is present only at the boundary $z = 0$, it will be included as a boundary condition rather than being included in Eq. (3.3).

Since this treatment is an extension of the Feinberg-Galanin treatment, some of Feinberg's notation will be adopted. Define the thermal constant γ_k as the ratio of the total net current of thermal neutrons into the k th rod to the value of the thermal neutron flux at the surface of the k th rod. $\phi_s(\underline{r}_k, t)$ will be used for the thermal neutron flux at the

surface of the k^{th} rod. The neutron yield per thermal neutron absorption, η , will be assumed to be the same for all rods. With the above assumptions and definitions, $S(\underline{r}, u, t)$ and $A(\underline{r}, t)$ become

$$S(\underline{r}, u, t) = \sum_k \delta(u) \frac{\Sigma_s(0)}{\Sigma_t(0)} \eta \gamma_k \phi_s(\underline{r}_k, t) \delta(\underline{r} - \underline{r}_k) \quad (3.4)$$

and

$$A(\underline{r}, t) = \sum_k \gamma_k \phi_s(\underline{r}_k, t) \delta(\underline{r} - \underline{r}_k) . \quad (3.5)$$

The ratio of the scattering to total cross sections at the source lethargy in Eq. (3.4) represents the probability of a neutron starting the slowing-down process.

Due to the separability of space and time for the flux, slowing-down density, and source term, Eqs. (3.1), (3.2), and (3.4) may be combined to give

$$\begin{aligned} & \left[-D(u) \nabla^2 + \Sigma_a(u) + \frac{i\omega}{v(u)} + \xi \Sigma_t(u) \frac{\partial}{\partial u} \right] q(\underline{r}, u) \\ &= \xi \Sigma_t(u) \frac{\Sigma_s(0)}{\Sigma_t(0)} \eta \sum_k \delta(u) \gamma_k \phi_s(\underline{r}_k) \delta(\underline{r} - \underline{r}_k) . \end{aligned} \quad (3.6)$$

Similarly, Eqs. (3.3) and (3.5) become

$$\left[-D_s \nabla^2 + \Sigma_{as} + \frac{i\omega}{v_s} \right] \phi_s(\underline{r}) = q(\underline{r}, u_s) - \sum_k \gamma_k \phi_s(\underline{r}_k) \delta(\underline{r} - \underline{r}_k) . \quad (3.7)$$

The boundary conditions on $\phi_s(\underline{r})$ will be the same as those used for the thermal neutron flux previously; the boundary conditions on $q(\underline{r}, u)$ will be identical, for $u > 0$, except that at $z = 0$, $q(\underline{r}, u)$ will be taken as zero on all boundaries. This corresponds to assuming that $\phi(\underline{r}, u) = 0$ at all boundaries for $u > 0$, which is consistent with the thermal neutron flux assumptions.

Defining

$$\beta(u, \omega) \equiv \frac{\Sigma_a(u) + \frac{i\omega}{v(u)}}{\xi \Sigma_t(u)} , \quad (3.8)$$

Eq. (3.6) may be written as

$$\begin{aligned} & \left[-\frac{D(u)}{\xi \Sigma_t(u)} \nabla^2 + \beta(u, \omega) + \frac{\partial}{\partial u} \right] q(\underline{r}, u) \\ &= \frac{\Sigma_s(0)}{\Sigma_t(0)} \eta \sum_k \delta(u) \gamma_k \phi_s(\underline{r}_k) \delta(\underline{r} - \underline{r}_k) . \quad (3.9) \end{aligned}$$

Multiplying through Eq. (3.9) by the integrating factor

$$\exp \left[\int_0^u \beta(u', \omega) du' \right] , \quad \text{Eq. (3.9) may be written as}$$

$$\begin{aligned}
& - \frac{D(u)}{\xi \Sigma_t(u)} \nabla^2 q(\underline{r}, u) e^{\circ} + \frac{\partial}{\partial u} \left[q(\underline{r}, u) e^{\circ} \right] \\
& = e^{\circ} \int^u \beta(u', \omega) du' \frac{\Sigma_s(0)}{\Sigma_t(0)} \eta \sum_k \delta(u) \gamma_k \phi_s(\underline{r}_k) \delta(\underline{r} - \underline{r}_k) . \quad (3.10)
\end{aligned}$$

In order to simplify the notation, define the Fermi age, τ , from

$$\frac{d\tau}{du} \equiv \frac{D(u)}{\xi \Sigma_t(u)} \quad \text{with } \tau(u=0) = 0 \quad (3.11)$$

and also define a frequency-dependent resonance escape probability, $p(u, \omega)$, as

$$p(u, \omega) \equiv e^{\circ} \int^u \beta(u', \omega) du' \quad (3.12)$$

Notice that the above definition is similar to the usual resonance escape probability except that an additional $1/v$ absorber has been added by the oscillating source.

With the two definitions [Eqs. (3.11) and (3.12)] Eq. (3.10) becomes

$$\begin{aligned}
& \frac{1}{p(\tau, \omega)} \nabla^2 q(\underline{r}, \tau) - \frac{\partial}{\partial \tau} \left[\frac{q(\underline{r}, \tau)}{p(\tau, \omega)} \right] \\
& = - \frac{1}{p(\tau, \omega)} \frac{\Sigma_s(0)}{\Sigma_t(0)} \eta \sum_k \delta(\tau) \gamma_k \phi_s(\underline{r}_k) \delta(\underline{r} - \underline{r}_k) . \quad (3.13)
\end{aligned}$$

The partial with respect to the Fermi age will be eliminated by using the Laplace transform. Defining

$$\theta(\underline{r}, s) \equiv \int_0^\infty e^{-\tau s} \frac{q(\underline{r}, \tau)}{p(\tau, \omega)} d\tau , \quad (3.14)$$

Eq. (3.13) becomes

$$\nabla^2 \theta(\underline{r}, s) - s \theta(\underline{r}, s) + \frac{q(\underline{r}, 0)}{p(0, \omega)} = - \frac{\Sigma_s(0)}{\Sigma_t(0)} \eta \sum_k \gamma_k \phi_s(\underline{r}_k) \delta(\underline{r} - \underline{r}_k) . \quad (3.15)$$

The term $q(\underline{r}, 0)$ is zero since $q(\underline{r}, 0)$ was incorporated into the original equation and is, of course, the negative of the right-hand side of Eq. (3.15). If it had been chosen that this source be introduced as a boundary condition, it could have been omitted from the original equation and have been introduced naturally at this point.

The obvious step at this point, consistent with previous methods, is to expand θ in the y eigenfunctions given in Eq. (2.2), which were determined by Eq. (2.1) and the boundary conditions of symmetry and $\psi_k(\pm b) = 0$. The required expansions are

$$\theta(\underline{r}, s) = \sum_\ell \theta_\ell(x, z, s) \psi_\ell(y) \quad (3.16)$$

and

$$\phi_s(\underline{r}) = \sum_\ell \phi_\ell(x, z) \psi_\ell(y) . \quad (3.17)$$

For future use, it should be noted that Eq. (3.16) implies that

$$\frac{q(r, \tau)}{p(\tau, \omega)} = \sum_{\ell} Q_{\ell}(x, z, \tau) \psi_{\ell}(y); \quad (3.18)$$

Eq. (3.16) may, in fact, be obtained from Eq. (3.18) by Laplace-transforming both sides of Eq. (3.18), where Q_{ℓ} is the inverse transform of θ_{ℓ} .

Inserting Eqs. (3.16) and (3.17) into Eq. (3.15) and operating with

$$\int_{-b}^b \psi_j(y) dy \text{ gives}$$

$$\left[\frac{\partial^2}{\partial x^2} + \frac{\partial^2}{\partial z^2} - (s + B_{\ell}^2) \right] \theta_{\ell}(x, z, s) = - \frac{\Sigma_s(0)}{\Sigma_t(0)} \eta \sum_k \gamma_k \delta(x - x_k) \delta(z - z_k) \phi_{\ell}(x, z), \quad (3.19)$$

where

$$B_{\ell}^2 \equiv \left[\frac{(2\ell - 1)\pi}{2b} \right]^2. \quad (3.20)$$

Now $\theta_{\ell}(x, z, s)$ is expanded in the x eigenfunctions of Eq. (2.14), defined in Eq. (2.13):

$$\theta_{\ell}(x, z, s) = \sum_j \left\{ \theta_j(z, s) \frac{1}{\sqrt{a}} \cos \frac{(2j - 1)\pi x}{2a} + \theta_j'(z, s) \frac{1}{\sqrt{a}} \sin \frac{j\pi x}{a} \right\}. \quad (3.21)$$

Inserting Eq. (3.21) into Eq. (3.19) results in

$$\begin{aligned}
& \sum_j \theta_j \left(-\frac{1}{\sqrt{a}} \right) \left[\frac{(2j-1)\pi}{2a} \right]^2 \cos \frac{(2j-1)\pi x}{2a} + \sum_j \theta'_j \left(-\frac{1}{\sqrt{a}} \right) \left[\frac{j\pi}{a} \right]^2 \sin \frac{j\pi x}{a} \\
& + \sum_j \frac{\partial^2 \theta_j}{\partial z^2} \frac{1}{\sqrt{a}} \cos \frac{(2j-1)\pi x}{2a} + \sum_j \frac{\partial^2 \theta'_j}{\partial z^2} \frac{1}{\sqrt{a}} \sin \frac{j\pi x}{a} \\
& - (s + B_\ell^2) \sum_j \left\{ \theta_j \frac{1}{\sqrt{a}} \cos \frac{(2j-1)\pi x}{2a} + \theta'_j \frac{1}{\sqrt{a}} \sin \frac{j\pi x}{a} \right\} \\
& = - \frac{\Sigma_s(0)}{\Sigma_t(0)} \eta \sum_k \gamma_k \delta(x - x_k) \delta(z - z_k) \phi_\ell(x, z) . \quad (3.22)
\end{aligned}$$

Operating on Eq. (3.22) with $\int_{-a}^a \frac{1}{\sqrt{a}} \cos \frac{(2m-1)\pi x}{2a} dx$ gives

$$\begin{aligned}
& - \theta_j(z, s) \left[\frac{(2j-1)\pi}{2a} \right]^2 + \frac{\partial^2 \theta_j(z, s)}{\partial z^2} - (s + B_\ell^2) \theta_j(z, s) \\
& = - \frac{\Sigma_s(0)}{\Sigma_t(0)} \eta \sum_k \gamma_k \delta(z - z_k) \frac{1}{\sqrt{a}} \cos \frac{(2j-1)\pi x_k}{2a} \phi_\ell(x_k, z) . \quad (3.23)
\end{aligned}$$

Similarly, operating on Eq. (3.22) with $\int_{-a}^a \frac{1}{\sqrt{a}} \sin \frac{m\pi x}{a} dx$ gives

$$\begin{aligned}
& - \theta'_j(z, s) \left[\frac{j\pi}{a} \right]^2 + \frac{\partial^2 \theta'_j(z, s)}{\partial z^2} - (s + B_\ell^2) \theta'_j(z, s) \\
& = - \frac{\Sigma_s(0)}{\Sigma_t(0)} \eta \sum_k \gamma_k \delta(z - z_k) \frac{1}{\sqrt{a}} \sin \frac{j\pi x_k}{a} \phi_\ell(x_k, z) . \quad (3.24)
\end{aligned}$$

Defining

$$\mu^2 \equiv s + B_\ell^2 + \left[\frac{(2j-1)\pi}{2a} \right]^2 \quad (3.25)$$

and

$$\xi^2 \equiv s + B_\ell^2 + \left[\frac{j\pi}{a} \right]^2 , \quad (3.26)$$

Eqs. (3.23) and (3.24) may be rewritten as

$$\begin{aligned} & \frac{\partial^2 \theta_j(z, s)}{\partial z^2} - \mu^2 \theta_j(z, s) \\ &= - \frac{\Sigma_s(0)}{\Sigma_t(0)} \eta \sum_k \gamma_k \delta(z - z_k) \frac{1}{\sqrt{a}} \cos \frac{(2j-1)\pi x_k}{2a} \phi_\ell(x_k, z) \end{aligned} \quad (3.27)$$

and

$$\begin{aligned} & \frac{\partial^2 \theta_j'(z, s)}{\partial z^2} - \xi^2 \theta_j'(z, s) \\ &= - \frac{\Sigma_s(0)}{\Sigma_t(0)} \eta \sum_k \gamma_k \delta(z - z_k) \frac{1}{\sqrt{a}} \sin \frac{j\pi x_k}{a} \phi_\ell(x_k, z) . \end{aligned} \quad (3.28)$$

The variable s has now been hidden in μ and ξ ; so the above two equations are effectively one dimensional. It may also be noted that Eqs. (3.27) and (3.28) are Green's function equations. Consider the boundary conditions which are appropriate for these equations. Aside from the usual conditions of continuity at $z = z_k$ and the discontinuity in the first derivative at

that point, the appropriate conditions must be derived from the original z -axis condition on $q(\underline{r}, \tau)$, which are

$$q(\underline{r}, \tau) \Big|_{z=0} = \lim_{z \rightarrow \infty} q(\underline{r}, \tau) = 0; \quad \tau \neq 0 . \quad (3.29)$$

Using these relations along with the expansions that have been utilized, Eqs. (3.16), (3.18), and (3.21), results in the following boundary conditions for Eqs. (3.27) and (3.28):

$$\theta_j(z, s) \Big|_{z=0} = \lim_{z \rightarrow \infty} \theta_j(z, s) = 0 \quad (3.30)$$

and

$$\theta_j'(z, s) \Big|_{z=0} = \lim_{z \rightarrow \infty} \theta_j'(z, s) = 0 . \quad (3.31)$$

Except for the fact that the function itself, rather than the first derivative, is zero at $z = 0$, we now have a problem identical to the one-dimensional Green's functions of Chapters I and II. By following procedures identical to those used in Chapter I, it is easily shown that the solution to

$$\frac{d^2\theta(z, z_0)}{dz^2} - K^2 \theta(z, z_0) = -\delta(z - z_0) \quad (3.32)$$

with boundary conditions

$$\theta(z, z_0) \Big|_{z=0} = \lim_{z \rightarrow \infty} \theta(z, z_0) = 0 \quad (3.33)$$

is

$$\begin{aligned}\theta(z, z_0) &= \frac{e^{-Kz} \sinh K z_0}{K}, \quad z > z_0, \\ &= \frac{e^{-Kz_0}}{K} \sinh K z, \quad z < z_0.\end{aligned}\tag{3.34}$$

Comparing Eqs. (2.25) and (2.28) with Eqs. (3.32) and (3.34) shows that the change in boundary condition has simply resulted in the cosh being replaced by the sinh. By writing the sinh as the difference of two exponentials in Eq. (3.34), it is easily seen that the two solutions may be combined into a form which will prove to be useful later:

$$\theta(z, z_0) = \frac{e^{-K|z-z_0|}}{2K} - \frac{e^{-K(z+z_0)}}{2K}. \tag{3.35}$$

Using this result, the solutions to Eqs. (3.27) and (3.28) may now be immediately written down, being

$$\begin{aligned}\theta_j(z, s) &= \frac{\Sigma_s(0)}{\Sigma_t(0)} \frac{n}{2\mu} \sum_k \left[e^{-\mu|z-z_k|} - e^{-\mu(z+z_k)} \right] \\ &\quad \gamma_k \frac{1}{\sqrt{a}} \cos \frac{(2j-1)\pi x_k}{2a} \phi_\ell(x_k, z_k)\end{aligned}\tag{3.36}$$

and

$$\begin{aligned}\theta_j'(z, s) &= \frac{\Sigma_s(0)}{\Sigma_t(0)} \frac{n}{2\xi} \sum_k \left[e^{-\xi|z-z_k|} - e^{-\xi(z+z_k)} \right] \\ &\quad \gamma_k \frac{1}{\sqrt{a}} \sin \frac{j\pi x_k}{a} \phi_\ell(x_k, z_k).\end{aligned}\tag{3.37}$$

Inserting Eqs. (3.36) and (3.37) into Eq. (3.21) gives

$$\begin{aligned} \theta_\ell(x, z, s) &= \frac{\Sigma_s(0)}{\Sigma_t(0)} \frac{1}{2a} \sum_j \sum_k \gamma_k \left\{ \frac{e^{-\mu|z-z_k|} - e^{-\mu(z+z_k)}}{\mu} \right. \\ &\quad \cos \frac{(2j-1)\pi x}{2a} \cos \frac{(2j-1)\pi x_k}{2a} \phi_\ell(x_k, z_k) \\ &\quad \left. + \frac{e^{-\xi|z-z_k|} - e^{-\xi(z+z_k)}}{\xi} \sin \frac{j\pi x}{a} \sin \frac{j\pi x_k}{a} \phi_\ell(x_k, z_k) \right\} . \end{aligned} \quad (3.38)$$

The next step is to inverse-Laplace-transform Eq. (3.38), obtaining the expansion coefficient in Eq. (3.18), which is

$$Q_\ell(x, z, \tau) = \mathcal{L}^{-1} \theta_\ell(x, z, s) . \quad (3.39)$$

Rewriting the definitions of μ and ξ as

$$\mu^2 = s + B_{\ell j}^2 \quad \text{and} \quad \xi^2 = s + B_{\ell j}^{12} , \quad (3.40)$$

where

$$B_{\ell j}^2 = \left[\frac{(2\ell-1)\pi}{2b} \right]^2 + \left[\frac{(2j-1)\pi}{2a} \right]^2 \quad \text{and} \quad B_{\ell j}^{12} = \left[\frac{(2\ell-1)\pi}{2b} \right]^2 + \left[\frac{j\pi}{a} \right]^2 , \quad (3.41)$$

it is evident that each term to be inverse-transformed is of the form

$$\frac{e^{-\sqrt{s+\alpha} z^*}}{\sqrt{s+\alpha}} , \quad (3.42)$$

which has the inverse

$$\frac{e^{-\alpha\tau}}{\sqrt{\pi\tau}} e^{-(z^*/4\tau)} \quad \text{for } z^* > 0 \quad . \quad (3.43)$$

Using Eq. (3.41), the inverse transform of Eq. (3.38), $Q_\ell(x, z, \tau)$, is

$$Q_\ell(x, z, \tau) = \frac{\Sigma_s(0)}{\Sigma_t(0)} \frac{\eta}{2a\sqrt{\pi\tau}} \sum_j \sum_k \gamma_k \left[e^{-(z-z_k)^2/4\tau} - e^{-(z+z_k)^2/4\tau} \right] \\ \left\{ e^{-B_{\ell j}^2 \tau} \cos \frac{(2j-1)\pi x_k}{2a} \cos \frac{(2j-1)\pi x_k}{2a} + e^{-B_{\ell j}^2 \tau} \sin \frac{j\pi x_k}{a} \sin \frac{j\pi x_k}{a} \right\} \\ \phi_\ell(x_k, z_k) \quad . \quad (3.44)$$

Returning now to the thermal-neutron diffusion equation, insert Eqs. (3.17) and (3.18) [with τ_s replacing τ in Eq. (3.18)] into Eq. (3.7) and

operate with $\int_{-b}^b \psi_j(y) dy$ to obtain

$$\left[-D_s \left(\frac{\partial^2}{\partial x^2} + \frac{\partial^2}{\partial z^2} \right) + \left(D_s B_{\ell j}^2 + \Sigma_{as} + \frac{i\omega}{v_s} \right) \right] \phi_\ell(x, z) \\ = p(\tau_s, \omega) Q_\ell(x, z, \tau_s) - \sum_k \gamma_k \phi_\ell(x, z) \delta(x - x_k) \delta(z - z_k) \quad . \quad (3.45)$$

Using the expansions

$$\phi_\ell(x, z) = \frac{1}{\sqrt{a}} \sum_j \left[\phi_{j\ell}(z) \cos \frac{(2j-1)\pi x}{2a} + \phi'_{j\ell}(z) \sin \frac{j\pi x}{a} \right] \quad (3.46)$$

and

$$Q_\ell(x, z, \tau_s) = \frac{1}{\sqrt{a}} \sum_j \left[Q_j(z, \tau_s) \cos \frac{(2j - 1)\pi x}{2a} + Q'_j(z, \tau_s) \sin \frac{j\pi x}{a} \right] \quad (3.47)$$

in Eq. (3.45) and operating with $\int_{-a}^a \frac{1}{\sqrt{a}} \cos \frac{(2j - 1)\pi x}{2a} dx$ gives

$$\begin{aligned} D_s \left[\frac{(2j - 1)\pi}{2a} \right]^2 \phi_{j\ell}(z) - D_s \frac{d^2 \phi_{j\ell}(z)}{dz^2} + \left[D_s B_\ell^2 + \Sigma_{as} + \frac{i\omega}{v_s} \right] \phi_{j\ell}(z) \\ = p(\tau_s, \omega) Q_j(z, \tau_s) - \frac{1}{\sqrt{a}} \sum_k \gamma_k \cos \frac{(2j - 1)\pi x_k}{2a} \phi_\ell(x_k, z) \delta(z - z_k) . \quad (3.48) \end{aligned}$$

Similarly expanding and operating with $\int_{-a}^a \frac{1}{\sqrt{a}} \sin \frac{j\pi x}{a} dx$ gives

$$\begin{aligned} D_s \left[\frac{j\pi}{a} \right]^2 \phi'_{j\ell}(z) - D_s \frac{d^2 \phi'_{j\ell}(z)}{dz^2} + \left[D_s B_\ell^2 + \Sigma_{as} + \frac{i\omega}{v_s} \right] \phi'_{j\ell}(z) \\ = p(\tau_s, \omega) Q'_j(z, \tau_s) - \frac{1}{\sqrt{a}} \sum_k \gamma_k \sin \frac{j\pi x_k}{a} \phi_\ell(x_k, z) \delta(z - z_k) . \quad (3.49) \end{aligned}$$

Defining

$$K^2 \equiv B_{\ell j}^2 + \frac{\Sigma_{as} + \frac{i\omega}{v_s}}{D_s} \quad (3.50)$$

and

$$K'^2 \equiv B_{\ell j}^{\prime 2} + \frac{\Sigma_{as} + \frac{i\omega}{v_s}}{D_s} , \quad (3.51)$$

Eqs. (3.48) and (3.49) may be written as

$$\begin{aligned} \frac{d^2 \phi_{j\ell}(z)}{dz^2} - K'^2 \phi_{j\ell}(z) &= \frac{-p(\tau_s, \omega)}{D_s} Q_j(z, \tau_s) \\ &+ \frac{1}{D\sqrt{a}} \sum_k \gamma_k \cos \frac{(2j-1)\pi x_k}{2a} \phi_\ell(x_k, z) \delta(z - z_k) \end{aligned} \quad (3.52)$$

and

$$\begin{aligned} \frac{d^2 \phi_{j\ell}'(z)}{dz^2} - K'^2 \phi_{j\ell}'(z) &= - \frac{p(\tau_s, \omega)}{D_s} Q_j'(z, \tau_s) \\ &+ \frac{1}{D\sqrt{a}} \sum_k \gamma_k \sin \frac{j\pi x_k}{a} \phi_\ell(x_k, z) \delta(z - z_k) . \end{aligned} \quad (3.53)$$

Comparison of the expansion, Eq. (3.47), with Eq. (3.44) shows that

$$\begin{aligned} Q_j(z, \tau_s) &= \frac{\Sigma_s(0)}{\Sigma_t(0)} \frac{\eta e^{-B_{\ell j}^2 \tau_s}}{2\sqrt{\pi a \tau_s}} \sum_k \gamma_k \left[e^{-\frac{(z-z_k)^2}{4\tau_s}} - e^{-\frac{(z+z_k)^2}{4\tau_s}} \right] \\ &\cos \frac{(2j-1)\pi x_k}{2a} \phi_\ell(x_k, z_k) \end{aligned} \quad (3.54)$$

and

$$Q_j^!(z, \tau_s) = \frac{\Sigma_s(0)}{\Sigma_t(0)} \frac{\eta e^{-B_{\ell j}^2 \tau_s}}{2\sqrt{\pi a \tau_s}} \sum_k \gamma_k \left[e^{-\frac{(z-z_k)^2}{4\tau_s}} - e^{-\frac{(z+z_k)^2}{4\tau_s}} \right] \sin \frac{j\pi x_k}{a} \phi_\ell(x_k, z_k) . \quad (3.55)$$

Since Eq. (3.52) along with Eq. (3.54) is so similar to Eqs. (3.53) and (3.55), attention will be restricted to the former set; then the latter set will be handled by comparison.

Equations (3.52) and (3.54) may be combined as

$$\frac{d^2 \phi_{j\ell}(z)}{dz^2} - k^2 \phi_{j\ell}(z) = - A_{\ell j} \sum_k F_{jk}(z, z_k) + \sum_k H_{jk}(z) \delta(z - z_k) , \quad (3.56)$$

where

$$A_{\ell j} \equiv \frac{\Sigma_s(0) \eta p(\tau_s, \omega) e^{-B_{\ell j}^2 \tau_s}}{\Sigma_t(0) 2 D_s \sqrt{\pi a \tau_s}} , \quad (3.57)$$

$$F_{jk}(z, z_k) \equiv \gamma_k \left[e^{-\frac{(z-z_k)^2}{4\tau_s}} - e^{-\frac{(z+z_k)^2}{4\tau_s}} \right] \cos \frac{(2j-1)\pi x_k}{2a} \phi_\ell(x_k, z_k) , \quad (3.58)$$

$$H_{jk}(z) \equiv \frac{1}{D_s \sqrt{a}} \gamma_k \cos \frac{(2j-1)\pi x_k}{2a} \phi_\ell(x_k, z) . \quad (3.59)$$

Equation (3.56) is virtually identical to Eq. (1.30) and has essentially the same boundary conditions, so that the Green's function of

Chapter I may be used to convert Eq. (3.56) to an integral equation. The appropriate Green's function is determined by

$$\frac{\partial^2 G_j(z, \xi)}{\partial z^2} - K^2 G_j(z, \xi) = -\delta(z - \xi) \quad (3.60)$$

and the usual homogeneous boundary conditions. The solution to Eq. (3.60), from previous results, is

$$\begin{aligned} G_j(z, \xi) &= \frac{e^{-Kz}}{K} \frac{\cosh K\xi}{\cosh K\xi} , \quad z > \xi , \\ &= \frac{e^{-K\xi}}{K} \frac{\cosh Kz}{\cosh K\xi} , \quad z < \xi . \end{aligned} \quad (3.61)$$

As before, the integral equation for $\phi_{j\ell}(z)$ is found by forming

$$\int_0^\infty d\xi G_j(\xi, z) [Eq. (3.56)] - \int_0^\infty d\xi \phi_{j\ell}(\xi) [Eq. (3.60)], \text{ after reversing}$$

z and ξ in Eqs. (3.56) and (3.60). This result is

$$\begin{aligned} &\int_0^\infty d\xi \left[G_j(\xi, z) \frac{d^2 \phi_{j\ell}(\xi)}{d\xi^2} - \phi_{j\ell}(\xi) \frac{\partial^2 G_j(\xi, z)}{\partial \xi^2} \right] \\ &= -A_{\ell j} \int_0^\infty d\xi G_j(\xi, z) \sum_k F_{jk}(\xi, z_k) \\ &+ \int_0^\infty d\xi G_j(\xi, z) \sum_k H_{jk}(\xi) \delta(\xi - z_k) + \phi_{j\ell}(z) . \end{aligned} \quad (3.62)$$

An integration by parts may be performed on the integrals containing the derivatives and the integral containing H_{jk} may be completed, resulting in

$$\begin{aligned}\phi_{j\ell}(z) = & - \sum_k G_j(z_k, z) H_{jk}(z_k) + A_{\ell j} \int_0^\infty d\xi G_j(\xi, z) \sum_k F_{jk}(\xi, z_k) \\ & + \left[G_j(\xi, z) \frac{d\phi_{j\ell}(\xi)}{d\xi} - \phi_{j\ell}(\xi) \frac{\partial G_j(\xi, z)}{\partial \xi} \right]_0^\infty.\end{aligned}\quad (3.63)$$

Inserting the boundary conditions into the last term gives

$$\begin{aligned}\phi_{j\ell}(z) = & - \sum_k G_j(z_k, z) H_{jk}(z_k) + A_{\ell j} \int_0^\infty d\xi G_j(\xi, z) \sum_k F_{jk}(\xi, z_k) \\ & - G_j(\xi, z) \Big|_{\xi=0} \frac{d\phi_{j\ell}(\xi)}{d\xi} \Big|_{\xi=0}.\end{aligned}\quad (3.64)$$

Inserting $A_{\ell j}$ and H_{jk} and assuming that $z_{M'} \leq z \leq z_{M'+1}$, Eq. (3.64) becomes

$$\begin{aligned}\phi_{j\ell}(z) = & - \frac{e^{-Kz}}{K} \frac{d\phi_{j\ell}(\xi)}{d\xi} \Big|_{\xi=0} - \frac{1}{KD\sqrt{a}} \left\{ e^{-Kz} \sum_{k=1}^{M'} \cosh Kz_k \gamma_k \cos \frac{(2j-1)\pi x_k}{2a} \right. \\ & \left. \phi_\ell(x_k, z_k) + \cosh Kz \sum_{k=M'+1}^M e^{-Kz_k} \gamma_k \cos \frac{(2j-1)\pi x_k}{2a} \phi_\ell(x_k, z_k) \right\} \\ & + \frac{\Sigma_s(0) \eta p(\tau_s, \omega) e^{-B_{\ell j}^2 \tau_s}}{\Sigma_t(0) 2 K D_s \sqrt{\pi a \tau_s}} \left\{ e^{-Kz} \int_0^z d\xi \cosh K\xi \sum_k F_{jk}(\xi, z_k) \right. \\ & \left. + \cosh Kz \int_z^\infty d\xi e^{-K\xi} \sum_k F_{jk}(\xi, z_k) \right\}.\end{aligned}\quad (3.65)$$

It seems appropriate at this point, before continuing into the mathematical complexities, to simplify the notation in Eq. (3.65) and try to understand its physical significance. To this end call the first term in Eq. (3.65) $H_{jk\ell}$, since it represents the contribution which would be present in the homogeneous case. Also, redefine Eq. (3.58) and (3.59) as

$$F_{jk}(z, z_k) = \sqrt{\pi a \tau_s} M_k(z) w_{jk} \phi_\ell(x_k, z_k) \quad (3.66)$$

and

$$H_{jk}(z) = \frac{1}{D} w_{jk} \phi_\ell(x_k, z_k) , \quad (3.67)$$

where

$$M_k(z) = \frac{1}{\sqrt{\pi \tau_s}} \left[e^{-(z-z_k)^2/4\tau_s} - e^{-(z+z_k)^2/4\tau_s} \right] \quad (3.68)$$

and

$$w_{jk} = \frac{\gamma_k}{\sqrt{a}} \cos \frac{(2j-1)\pi x_k}{2a} . \quad (3.69)$$

w_{jk} is simply a weighting factor depending on the distance from the center line of the foil location. $M_k(z)$ is the slowing-down kernel for the particular geometry chosen, having an obvious resemblance to the infinite-medium Fermi-age kernel. Noticing the factor $1/\sqrt{\tau_s}$, it can be seen that the slowing-down kernel obtained for the present geometry resembles the plane source infinite-medium slowing-down kernel most closely. This is to be expected, since the problem was reduced to a semi-infinite, one-dimensional case.

Inserting Eqs. (3.66) and (3.67) into Eq. (3.65) and using the symmetric part of Eq. (3.46) and Eq. (3.61) results in

$$\begin{aligned} \phi_\ell(x, z) = & \sum_j W_j(x) H_{j\ell} - \sum_j \sum_k \frac{W_j(x)}{D} W_{jk} G_j(z_k, z) \phi_\ell(x_k, z_k) \\ & + \sum_j \sum_k \sqrt{\pi \tau_s} A_{j\ell} W_j(x) W_{jk} \phi_\ell(x_k, z_k) \int_0^\infty d\xi M_k(\xi) G_j(z_k, \xi) , \end{aligned} \quad (3.70)$$

where

$$W_j(x) = \frac{1}{\sqrt{a}} \cos \frac{(2j-1)\pi x}{2a} . \quad (3.71)$$

It should now be noted that the ℓ th mode of the flux distribution consists of the following parts: (a) the homogeneous term $\sum_j H_{j\ell}$, which represents the propagation of a neutron wave in a homogeneous system, (b) the absorbing part, the second term, which accounts for the heterogeneous absorption of the plates, and (c) the last term, which accounts for the production of fast neutrons by fissions in the plates, and their subsequent slowing down into the thermal group.

Returning to the mathematical manipulations, it now remains to evaluate the two integrals in Eq. (3.65), which are complicated by the fact that K is a complex quantity. The first integral may be written as

$$\int_0^z d\xi \cosh K\xi \sum_k \left\{ e^{-\frac{(\xi-z_k)^2}{4\tau_s}} - e^{-\frac{(\xi+z_k)^2}{4\tau_s}} \right\} E_{jk} , \quad (3.72)$$

where

$$E_{jk} \equiv \gamma_k \cos \frac{(2j - 1)\pi x_k}{2a} \phi_\ell(x_k, z_k) . \quad (3.73)$$

Expressing the cosh as the sum of exponentials and performing the squares in the exponentials, Eq. (3.72) may be reformulated as

$$\sum_k \frac{e^{-z_k^2/4\tau_s}}{2} \int_0^z d\xi \left(e^{K\xi} + e^{-K\xi} \right) e^{-\xi^2/4\tau_s} \\ \left(e^{\xi z_k/2\tau_s} - e^{-\xi z_k/2\tau_s} \right) E_{jk} \quad (3.74)$$

Multiplying and combining the various exponentials leads to

$$\sum_k \frac{e^{-z_k^2/4\tau_s}}{2} E_{jk} \int_0^z d\xi e^{-\xi^2/4\tau_s} \left[e^{[K+(z_k/2\tau_s)]\xi} - e^{[K-(z_k/2\tau_s)]\xi} \right. \\ \left. + e^{-[K-(z_k/2\tau_s)]\xi} - e^{-[K+(z_k/2\tau_s)]\xi} \right] . \quad (3.75)$$

By completing the squares in each of the exponentials, Eq. (3.75) may be rewritten as

$$\begin{aligned}
& \sum_k \frac{e^{-z_k^2/4\tau_s}}{2} E_{jk} \int_0^z d\xi \left\{ e^{-\left[\frac{\xi}{2\sqrt{\tau_s}} - \sqrt{\tau_s} \left(K+ \frac{z_k}{2\tau_s}\right)\right]^2} \tau_s \left(K+ \frac{z_k}{2\tau_s}\right)^2 \right. \\
& \quad - \left[\frac{\xi}{2\sqrt{\tau_s}} - \sqrt{\tau_s} \left(K- \frac{z_k}{2\tau_s}\right) \right]^2 \tau_s \left(K- \frac{z_k}{2\tau_s}\right)^2 \\
& \quad - e \left. + e \right. \\
& \quad - \left[\frac{\xi}{2\sqrt{\tau_s}} + \sqrt{\tau_s} \left(K- \frac{z_k}{2\tau_s}\right) \right]^2 \tau_s \left(K- \frac{z_k}{2\tau_s}\right)^2 \\
& \quad + e \left. - e \right. \\
& \quad - \left[\frac{\xi}{2\sqrt{\tau_s}} + \sqrt{\tau_s} \left(K+ \frac{z_k}{2\tau_s}\right) \right]^2 \tau_s \left(K+ \frac{z_k}{2\tau_s}\right)^2 \left. \right\} . \tag{3.76}
\end{aligned}$$

Each of the four integrals in Eq. (3.76) is of the form

$$e^{\tau_s \alpha^2} \int_0^z d\xi e^{-\left(\frac{\xi}{2\sqrt{\tau_s}} \pm \sqrt{\tau_s} \alpha\right)^2} \tag{3.77}$$

which becomes, upon changing the variable of integration to

$$w \equiv \frac{\xi}{2\sqrt{\tau_s}} \pm \sqrt{\tau_s} \alpha , \tag{3.78}$$

$$\begin{aligned}
& e^{\frac{\tau_s \alpha^2}{2}} \int_{\frac{z}{2\sqrt{\tau_s}} - \pm \sqrt{\tau_s} \alpha}^{\frac{z}{2\sqrt{\tau_s}} + \sqrt{\tau_s} \alpha} e^{-w^2} dw \\
& = e^{\frac{\tau_s \alpha^2}{2}} \sqrt{\pi \tau_s} \left(\frac{2}{\sqrt{\pi}} \int_0^{\frac{z}{2\sqrt{\tau_s}} + \sqrt{\tau_s} \alpha} e^{-w^2} dw - \frac{2}{\sqrt{\pi}} \int_0^{\pm \sqrt{\tau_s} \alpha} e^{-w^2} dw \right). \tag{3.79}
\end{aligned}$$

Recognizing the two integrals as error functions, Eq. (3.79) becomes

$$\begin{aligned}
& \sqrt{\pi \tau_s} e^{\frac{\tau_s \alpha^2}{2}} \left\{ \operatorname{erf} \left[\frac{z}{2\sqrt{\tau_s}} \pm \sqrt{\tau_s} \alpha \right] - \operatorname{erf} \left[\pm \sqrt{\tau_s} \alpha \right] \right\} \\
& = \sqrt{\pi \tau_s} e^{\frac{\tau_s \alpha^2}{2}} \left\{ \operatorname{erf} \left[\frac{z}{2\sqrt{\tau_s}} \pm \sqrt{\tau_s} \alpha \right] \mp \operatorname{erf} \left[\sqrt{\tau_s} \alpha \right] \right\}, \tag{3.80}
\end{aligned}$$

where the error function is defined as

$$\operatorname{erf}(x) \equiv \frac{2}{\sqrt{\pi}} \int_0^x e^{-t^2} dt. \tag{3.81}$$

The integrals of Eq. (3.76) now become

$$\begin{aligned}
& \sum_k E_{jk} \frac{e^{-z_k^2/4\tau_s}}{2} \sqrt{\pi\tau_s} \left[e^{\tau_s \left(K + \frac{z_k}{2\tau_s} \right)^2} \left\{ \operatorname{erf} \left[\frac{z}{2\sqrt{\tau_s}} - \sqrt{\tau_s} \left(K + \frac{z_k}{2\tau_s} \right) \right] \right. \right. \\
& \quad \left. \left. - \operatorname{erf} \left[\frac{z}{2\sqrt{\tau_s}} + \sqrt{\tau_s} \left(K + \frac{z_k}{2\tau_s} \right) \right] + 2 \operatorname{erf} \left[\sqrt{\tau_s} \left(K + \frac{z_k}{2\sqrt{\tau_s}} \right) \right] \right\} \\
& \quad + e^{\tau_s \left(K - \frac{z_k}{2\tau_s} \right)^2} \left\{ \operatorname{erf} \left[\frac{z}{2\sqrt{\tau_s}} + \sqrt{\tau_s} \left(K - \frac{z_k}{2\tau_s} \right) \right] \right. \\
& \quad \left. \left. - \operatorname{erf} \left[\frac{z}{2\sqrt{\tau_s}} - \sqrt{\tau_s} \left(K - \frac{z_k}{2\tau_s} \right) \right] - 2 \operatorname{erf} \left[\sqrt{\tau_s} \left(K - \frac{z_k}{2\tau_s} \right) \right] \right\} \right] . \tag{3.82}
\end{aligned}$$

The second integral in Eq. (3.65) is

$$\int_z^\infty d\xi e^{-K\xi} \sum_k \left\{ e^{-(\xi-z_k)^2/4\tau_s} - e^{-(\xi+z_k)^2/4\tau_s} \right\} E_{jk} , \tag{3.83}$$

which can be handled in a similar manner to give

$$\begin{aligned}
& \sum_k E_{jk} e^{-z_k^2/4\tau_s} \sqrt{\pi\tau_s} \left[e^{\tau_s \left(K - \frac{z_k}{2\tau_s} \right)^2} \left\{ 1 - \operatorname{erf} \left[\frac{z}{2\sqrt{\tau_s}} + \sqrt{\tau_s} \left(K - \frac{z_k}{2\tau_s} \right) \right] \right\} \right. \\
& \quad \left. - e^{\tau_s \left(K + \frac{z_k}{2\tau_s} \right)^2} \left\{ 1 - \operatorname{erf} \left[\frac{z}{2\sqrt{\tau_s}} + \sqrt{\tau_s} \left(K + \frac{z_k}{2\tau_s} \right) \right] \right\} \right] . \tag{3.84}
\end{aligned}$$

If the squares in the factors $\exp \left[\tau_s \left(K \pm \frac{z_k}{2\tau_s} \right)^2 \right]$ in Eqs. (3.82) and (3.84) are performed, a factor $\exp \left[z_k^2/4\tau_s \right]$ will result which will cancel the $\exp \left[-z_k^2/4\tau_s \right]$. The two remaining factors are $\exp \left[\pm K z_k \right]$ and $\exp \left[\tau_s K^2 \right]$, which can be taken out of the summation and combined with the factor $\exp \left[-B_{\ell j}^2 \tau_s \right]$.

Now the expressions for the two integrals, Eqs. (3.82) and (3.84), may be inserted into Eq. (3.65) to give the complete expression for $\phi_{jl}(z)$. Thus:

$$\phi_{jl}(z) = \frac{e^{-Kz}}{K} \left. \frac{d\phi_{jl}(\xi)}{d\xi} \right|_{\xi=0} - \frac{1}{K D_s \sqrt{a}} \left\{ e^{-Kz} \sum_{k=1}^{M'} \cosh K z_k \gamma_k \cos \frac{(2j-1)\pi x_k}{2a} \right.$$

$$\left. \phi_{\ell}(x_k, z_k) + \cosh Kz \sum_{k=M'+1}^M e^{-Kz_k} \gamma_k \cos \frac{(2j-1)\pi x_k}{2a} \phi_{\ell}(x_k, z_k) \right\}$$

$$+ \frac{\Sigma_s(0) \eta p(\tau_s, \omega) e^{(K^2 - B_{\ell j}^2) \tau_s}}{\Sigma_t(0) 2 K D_s \sqrt{a}} \left\{ \frac{e^{-Kz}}{2} \sum_{k=1}^M \left[e^{Kz_k} \left\{ \operatorname{erf} \left[\frac{z - z_k}{2\sqrt{\tau_s}} - \sqrt{\tau_s} K \right] \right. \right. \right.$$

$$\left. \left. \left. - \operatorname{erf} \left[\frac{z + z_k}{2\sqrt{\tau_s}} + \sqrt{\tau_s} K \right] \right] + 2 \operatorname{erf} \left[\frac{z_k}{2\sqrt{\tau_s}} + \sqrt{\tau_s} K \right] \right\} + e^{-Kz_k}$$

$$\left\{ \operatorname{erf} \left[\frac{z - z_k}{2\sqrt{\tau_s}} + \sqrt{\tau_s} K \right] - \operatorname{erf} \left[\frac{z + z_k}{2\sqrt{\tau_s}} - \sqrt{\tau_s} K \right] \right\}$$

$$- 2 \operatorname{erf} \left[- \frac{z_k}{2\sqrt{\tau_s}} + \sqrt{\tau_s} K \right] \} \right]$$

(continued on following page)

$$\begin{aligned}
 & + \cosh Kz \sum_{k=1}^M \left[e^{Kz_k} \left\{ \operatorname{erf} \left[\frac{z + z_k}{2\sqrt{\tau_s}} + \sqrt{\tau_s} K \right] - 1 \right\} \right. \\
 & \left. - e^{-Kz_k} \left\{ \operatorname{erf} \left[\frac{z - z_k}{2\sqrt{\tau_s}} + \sqrt{\tau_s} K \right] - 1 \right\} \right] \gamma_k \cos \frac{(2j-1)\pi x_k}{2a} \phi_\ell(x_k, z_k) . \quad (3.85)
 \end{aligned}$$

Equation (3.85) with Eq. (3.46) used for $\phi_\ell(x_k, z_k)$ is the complete solution to Eq. (3.52). $\phi'_{j\ell}(z)$, the solution to Eq. (3.53), is similar to Eq. (3.85) except that K' replaces K , $B'_{\ell j}$ replaces $B_{\ell j}$, and $\sin(j\pi x_k/a)$ replaces $\cos \frac{(2j-1)\pi x_k}{2a}$ wherever they appear. Equation (3.85) and the corresponding equation for $\phi'_{j\ell}(z)$ are inserted into Eq. (3.46), which in turn is inserted into Eq. (3.17) to give the complete expression for $\phi(\underline{r})$, the thermal neutron flux at any point in the medium.

It is instructive to see what happens to Eq. (3.85) when the age-diffusion theory is reduced to one-group diffusion. If no errors have been made, Eq. (3.85) should reduce to essentially the same form as Eq. (1.66). To do this, let $\tau_s \rightarrow 0$ and set $p(\tau_s, \omega) = 1$. As $\tau_s \rightarrow 0$, the arguments of all the error functions will approach the form $\frac{z \pm z_k}{2\sqrt{\tau_s}}$ or $\pm \frac{z_k}{2\sqrt{\tau_s}}$. Obviously all the arguments will approach $\pm\infty$ on the real axis, depending in some cases on whether $z < z_k$ or $z > z_k$. The error function for $\pm\infty$ is simply ± 1 , and so the last term in Eq. (3.85) becomes

$$\begin{aligned}
& \frac{\Sigma_s(0)}{\Sigma_t(0)} \frac{\eta}{2KD_s \sqrt{a}} \left\{ e^{-Kz} \sum_{k=1}^M \frac{e^{-z_k^2/4\tau_s}}{2} \left[e^{\tau_s \left(K + \frac{z_k}{2\tau_s} \right)^2} \right] \right. \\
& \quad \left. \left\{ \begin{array}{l} 2; z > z_k \\ 0; z < z_k \end{array} \right\} \right\} \\
& + e^{\tau_s \left(K - \frac{z_k}{2\tau_s} \right)^2} \left[\left\{ \begin{array}{l} 2; z > z_k \\ 0; z < z_k \end{array} \right\} \right] \gamma_k \cos \frac{(2j-1)\pi x_k}{2a} \phi_\ell(x_k, z_k) \\
& + \cosh Kz \sum_{k=1}^M e^{-z_k^2/4\tau_s} \left[e^{\tau_s \left(K - \frac{z_k}{2\tau_s} \right)^2} - e^{\tau_s \left(K - \frac{z_k}{2\tau_s} \right)^2} \right] \\
& \quad \left. \left\{ \begin{array}{l} 1; z > z_k \\ -1; z < z_k \end{array} \right\} \right] \\
& \quad \gamma_k \cos \frac{(2j-1)\pi x_k}{2a} \phi_\ell(x_k, z_k) . \tag{3.86}
\end{aligned}$$

With a little further manipulation Eq. (3.86) can be further reduced to the form

$$\begin{aligned}
& \frac{\Sigma_s(0) \eta}{\Sigma_t(0) D_s \sqrt{a}} \left\{ e^{-Kz} \sum_{k=1}^{M'} \cosh Kz_k \gamma_k \cos \frac{(2j-1)\pi x_k}{2a} \phi_\ell(x_k, z_k) \right. \\
& \quad \left. + \frac{\cosh Kz}{K} \sum_{k=M'+1}^M e^{-Kz_k} \gamma_k \cos \frac{(2j-1)\pi x_k}{2a} \phi_\ell(x_k, z_k) \right. . \tag{3.87}
\end{aligned}$$

Insertion of Eq. (3.87) into Eq. (3.85) reduces the latter equation to

$$\phi_{j\ell}(z) = -\frac{e^{-Kz}}{K} \left. \frac{d\phi_{j\ell}(\xi)}{d\xi} \right|_{\xi=0} + \left[\frac{\Sigma_s(0)}{\Sigma_t(0)} \eta - 1 \right] \frac{1}{D_s \sqrt{a}} \left\{ \frac{e^{-Kz}}{K} \right.$$

$$\sum_{k=1}^{M'} \cosh K z_k \gamma_k \cos \frac{(2j-1)\pi x_k}{2a} \phi_\ell(x_k, z_k) + \frac{\cosh Kz}{K}$$

$$\left. \sum_{k=M'+1}^M e^{-K z_k} \gamma_k \cos \frac{(2j-1)\pi x_k}{2a} \phi_\ell(x_k, z_k) \right\} . \quad (3.88)$$

The resemblance of Eq. (3.88) to Eq. (1.66) is obvious. Except for the differences in the shapes of the perturbing foils assumed in the two derivations, by following a procedure similar to that described at the end of Chapter II the equivalence of the two expressions can easily be shown.

CHAPTER IV

CALCULATIONAL RESULTS

Two computer codes were written to obtain numerical results from the analytical results of the previous chapters. The simpler of the two uses the results of Chapter I with no additional analytical simplifications. The second code uses the age-diffusion model developed in Chapter III, but several restrictions had to be made because of computer storage and numerical problems.

The simpler of the two codes performs the procedures given from Eq. (1.67) to the end of Chapter I. Computer storage limitations resulted in several limitations on variable sizes. M , the number of foils, was limited to 6; using the terminology of Eq. (1.67), L was limited to 10, Q was limited to 5, and the product LM was limited to 30. The output of the code consisted of $\phi_{11}(z)$ for up to 49 uniformly spaced values of z and the summation of all the flux modes for the same z values. These results were given by the code for any number of uniformly spaced frequencies of the driving source.

Since the one-group, one-dimensional computer code almost completely filled the computer core, it was obvious that the two-dimensional age-diffusion results could not be coded in their entirety. Two major simplifications were made. One was to restrict the foil positions and flux calculational points to the z axis ($x_k = x = 0$), thereby transforming the problem to a one-dimensional problem. This results in the x expansion,

Eq. (3.46), reducing to

$$\phi_\ell(0, z) = \frac{1}{\sqrt{a}} \sum_j \phi_{j\ell}(z) . \quad (4.1)$$

Equation (3.79) simplifies somewhat since the factor $\cos \frac{(2j - 1)\pi x_k}{2a}$

becomes unity, and since $\phi'_{j\ell}(z)$ is not used in Eq. (4.1), the equation corresponding to Eq. (3.79) for $\phi'_{j\ell}(z)$ is not needed. Substitution of Eq. (4.1), with z_k replacing z , into Eq. (3.85) along with replacing the cosine factors with unity gives the basic equation the code must handle as follows:

$$\begin{aligned} \phi_\ell(0, z) = & - \frac{1}{\sqrt{a}} \sum_j \left. \frac{e^{-Kz}}{K} \frac{d\phi_{j\ell}(\xi)}{d\xi} \right|_{\xi=0} - \frac{1}{D_s a} \\ & \sum_j \left\{ \frac{e^{-Kz}}{K} \sum_{k=1}^{M'} \gamma_k \cosh Kz_k \phi_\ell(0, z_k) + \frac{\cosh Kz}{K} \right. \\ & \left. \sum_{k=M'+1}^M \gamma_k e^{-Kz_k} \phi_\ell(0, z_k) \right\} + \frac{\Sigma_s(0) \eta p(\tau_s, \omega)}{\Sigma_t(0) 2 D_s a} \\ & \sum_j \frac{(K^2 - B_{j\ell}^2)^{\tau_s}}{K} \gamma_k \left\{ \frac{e^{-Kz}}{2} \sum_{k=1}^M \left[e^{Kz_k} \left\{ \operatorname{erf} \left[\frac{z - z_k}{2\sqrt{\tau_s}} + \sqrt{\tau_s} K \right] \right. \right. \right. \\ & \left. \left. \left. - \operatorname{erf} \left[\frac{z + z_k}{2\sqrt{\tau_s}} + \sqrt{\tau_s} K \right] \right] + 2 \operatorname{erf} \left[\frac{z_k}{2\sqrt{\tau_s}} + \sqrt{\tau_s} K \right] \right\} \\ & + e^{-Kz_k} \left\{ \operatorname{erf} \left[\frac{z - z_k}{2\sqrt{\tau_s}} + \sqrt{\tau_s} K \right] - \operatorname{erf} \left[\frac{z + z_k}{2\sqrt{\tau_s}} - \sqrt{\tau_s} K \right] \right\} \end{aligned}$$

$$\begin{aligned}
& -2 \operatorname{erf} \left[-\frac{z_k}{2\sqrt{\tau_s}} + \sqrt{\tau_s} K \right] \} \Bigg] + \cosh Kz \sum_{k=1}^M \\
& \left[e^{Kz_k} \left\{ \operatorname{erf} \left[\frac{z + z_k}{2\sqrt{\tau_s}} + \sqrt{\tau_s} K \right] - 1 \right\} - e^{-Kz_k} \right. \\
& \left. \left\{ \operatorname{erf} \left[\frac{z - z_k}{2\sqrt{\tau_s}} + \sqrt{\tau_s} K \right] - 1 \right\} \right] \phi_\ell(0, z_k) . \quad (4.2)
\end{aligned}$$

The only other simplification that was made was only the inclusion of the fundamental spatial mode in the source. Formally, this implies that Eqs. (1.13), (1.22), and (1.24) apply and that $S_{\ell m} = 0$ for $\ell > 1$ and $m > 1$. In practice, the higher ℓ values (x modes) could have been easily included, but to have included the higher m values (y modes) would have overloaded the computer core. This is not an insurmountable obstacle, since magnetic tape storage could have been used but this is a time-consuming and therefore expensive approach. Physically, including only the fundamental spatial mode seems justified since recent experimental work at the University of Florida indicates that a highly thermalized fundamental mode is experimentally feasible (10).

Using Eq. (4.2) rather than Eq. (1.66), the procedure outlined in Chapter I from Eq. (1.66) to the end of the chapter may be used to obtain the complete solution to the problem. This will be done later in this chapter, but, first, attention will be directed to two factors in Eq. (4.2) which have physical significance that has not been pointed out previously.

If Eq. (3.8) is inserted into Eq. (3.12), with the age to thermal, τ_s , replacing u , the result is

$$p(\tau_s, \omega) = e^{-\int_0^{\tau_s} \frac{\Sigma_a(u') du'}{\xi \Sigma_t(u')}} e^{-i\omega \int_0^{\tau_s} \frac{du'}{\xi \Sigma_t(u') v(u')}} . \quad (4.3)$$

Noting that the first integral in Eq. (4.3) is the usual resonance escape probability to thermal, $p(\tau_s)$ or $p(u_s)$, Eq. (4.3) may be written as

$$p(\tau_s, \omega) = p(\tau_s) e^{-i\omega T_s} , \quad (4.4)$$

where

$$T_s \equiv \int_0^{\tau_s} \frac{du'}{\xi \Sigma_t(u') v(u')} \quad (4.5)$$

or, in terms of the Fermi age,

$$T_s \equiv \int_0^{\tau_s} \frac{d\tau}{D(\tau) v(\tau)} . \quad (4.6)$$

Obviously, T_s has the units of time, and represents the time required for the neutron to slow down to thermal energy. The factor $\exp[-i\omega T_s]$ then represents the phase shift introduced by the slowing-down time.

The second factor in Eq. (4.2) which can be simplified is $\exp[(K^2 - B_{\ell j}^2)\tau_s]$. With the use of Eq. (3.50), this immediately becomes

$$e^{(K^2 - B_{\ell j}^2)\tau_s} = e^{\frac{\Sigma_{as} + \frac{i\omega}{v_s}}{D_s} \tau_s} \quad (4.7)$$

$$= e^{\frac{\Sigma_{as} \tau_s}{D_s}} e^{-i\omega \frac{\tau_s}{v_s D_s}} . \quad (4.8)$$

The term in the first exponential is the ratio of the age to thermal to the square of the diffusion length, τ_s/L^2 . Remembering that for a point source L^2 is one-sixth the mean square distance that a thermal neutron travels before being absorbed and that $\tau(u)$ is one-sixth the mean square distance that a neutron travels in attaining lethargy u , the ratio can be seen to be a measure of the distance traveled while slowing down relative to the distance traveled at thermal energy. Typical values for this ratio are 0.13 for graphite and 0.008 for D₂O.

Now returning to the actual calculational procedure, as before, the expansion, Eq. (4.1), must be truncated; i.e.,

$$\phi_\ell(0, z) = \frac{1}{\sqrt{a}} \sum_{j=1}^J \phi_{j\ell}(z) . \quad (4.9)$$

Because of the restriction of the source to the fundamental mode only, Eq. (4.9) simplifies further, since ℓ can only assume the value 1. Restricting j to 1 in $S_{j\ell}$ does not, of course, eliminate the higher j components in the flux since the perturbing foils generate higher x modes but they cannot generate higher y modes since the foils are assumed to extend the full length of the medium in the y direction. Equation (3.85) with

$$\frac{1}{\sqrt{a}} \sum_{j=1}^J \phi_{j1}(z_k) \text{ inserted for } \phi_\ell(x_k, z_k) \text{ and } \cos \frac{(2j - 1)\pi x_k}{2a} \text{ replaced by unity}$$

may now be written JM times for each of the J modes and for each of the M foils. This set of equations may then be solved simultaneously for the JM values of $\phi_{j1}(z_k)$. Writing these values as a vector,

$$\Phi^T = [\phi_{11}(z_1), \phi_{11}(z_2), \dots, \phi_{11}(z_M), \phi_{21}(z_1), \dots, \phi_{J1}(z_M)] , \quad (4.10)$$

the set of JM equations may be put into matrix form, as before. That is,

$$[A] \Phi + [I] \Phi = B , \quad (4.11)$$

where B is the vector of source terms, $[I]$ is the identity matrix, and $[A]$ is the matrix containing the Green's functions connecting the foils. B may be written as

$$B^T = \left[\alpha_{11} e^{-K_{11} z_1}, \dots \alpha_{11} e^{-K_{11} z_M}, 0 \dots 0 \right] , \quad (4.12)$$

where

$$\alpha_{11} \equiv \frac{S_{11}}{2DK_{11}} . \quad (4.13)$$

The $[A]$ matrix is defined, as before, by partitioning it into J^2 submatrices, each M by M . The n,p element of the I,K submatrix is given by

$$(A_{I,K})_{n,p} = \beta_{Il}(z_p) \cosh K_{Il} z_p e^{-K_{Il} z_n} - \Delta_{Il}(R_{Il})_{n,p}, \quad \text{for } n > p , \quad (4.14)$$

$$= \beta_{Il}(z_p) \cosh K_{Il} z_n e^{-K_{Il} z_p} - \Delta_{Il}(R_{Il})_{n,p}, \quad \text{for } n < p , \quad (4.15)$$

where

$$\beta_{Il}(z_p) \equiv \frac{\gamma_p}{K_{Il} Da} , \quad (4.16)$$

$$\Delta_{Il} \equiv \frac{\Sigma_s(0)}{\Sigma_t(0)} \frac{\eta_p(\tau_s, \omega) e^{\frac{\Sigma_{as} + \frac{i\omega}{V_s}}{D_s} \tau_s}}{2 D_s a K_{Il}} , \quad (4.17)$$

$$\begin{aligned}
 (R_{II})_{n,p} &\equiv e^{-K_{II}(z_n - z_p)} \frac{\gamma_p}{2} \left\{ (A1) - (A2) + 2(A3) \right\} \\
 &+ e^{-K_{II}(z_n + z_p)} \frac{\gamma_p}{2} \left\{ (A4) - (A5) - 2(A6) \right\} \\
 &+ \cosh K_{II} z_p \left\{ e^{K_{II} z_p} [(A2) - 1] - e^{-K_{II} z_p} [(A4) - 1] \right\}, \quad (4.18)
 \end{aligned}$$

$$(A1) = \operatorname{erf} \left[\frac{z_n - z_p}{2\sqrt{\tau_s}} - \sqrt{\tau_s} K_{II} \right], \quad (4.19)$$

$$(A2) = \operatorname{erf} \left[\frac{z_n + z_p}{2\sqrt{\tau_s}} + \sqrt{\tau_s} K_{II} \right], \quad (4.20)$$

$$(A3) = \operatorname{erf} \left[\frac{z_p}{2\sqrt{\tau_s}} + \sqrt{\tau_s} K_{II} \right], \quad (4.21)$$

$$(A4) = \operatorname{erf} \left[\frac{z_n - z_p}{2\sqrt{\tau_s}} + \sqrt{\tau_s} K_{II} \right], \quad (4.22)$$

$$(A5) = \operatorname{erf} \left[\frac{z_n + z_p}{2\sqrt{\tau_s}} - \sqrt{\tau_s} K_{II} \right], \quad (4.23)$$

$$(A6) = \operatorname{erf} \left[-\frac{z_p}{2\sqrt{\tau_s}} + \sqrt{\tau_s} K_{II} \right]. \quad (4.24)$$

The vector Φ is obtained from

$$\Phi = \left[[A] + [I] \right]^{-1} B. \quad (4.25)$$

The elements of Φ are inserted into Eq. (3.85) with the previously mentioned simplifications, which is in turn inserted into Eq. (4.9) to give the complete answer to $\phi_1(0, z)$. The entire thermal neutron flux is obtained by using Eq. (3.17), which gives

$$\phi_s(0, 0, z) = \frac{1}{\sqrt{b}} \quad \phi_1(0, z) = \frac{1}{\sqrt{ab}} \sum_{j=1}^J \phi_{jl}(z) \quad . \quad (4.26)$$

Since the representation of the flux is by expansion in eigenfunctions, an important characteristic of the numerical calculations is the rate of convergence with increasing numbers of the eigenfunctions, or spatial modes. Figures 2 and 3 show flux amplitude versus distance along the z axis with 1, 2, 4, and 10 spatial modes and with the source modulated at 100 and 1000 cps, respectively. The model is the one-group representation of Chapter I with the geometry shown in Fig. 1. One cadmium strip, $0.0508 \times 1 \times 71.12$ cm, is positioned 8.89 cm from the end of a graphite assembly 44.45×71.12 cm, the dimensions of one of the experimental facilities available at the University of Florida. In addition to the curves shown in Figs. 2 and 3, calculations were performed with 6 and 8 spatial modes. At the position of slowest convergence, which is in the neighborhood of the cadmium foil, the ratios of the 6- and 8-mode results to the 10-mode results are approximately 15 and 6%, respectively, for both 100- and 1000-cps source frequencies. Figure 4 shows the phase lag versus z for 100 cps, corresponding to Fig. 2. In this case the change from 6 to 10 modes and from 8 to 10 modes is approximately 5 and 2%, respectively. Figure 5 is the phase lag versus z for 1000 cps, corresponding to Fig. 3. The convergence is faster for this case, approximately 2.5 and 1% for 6 to

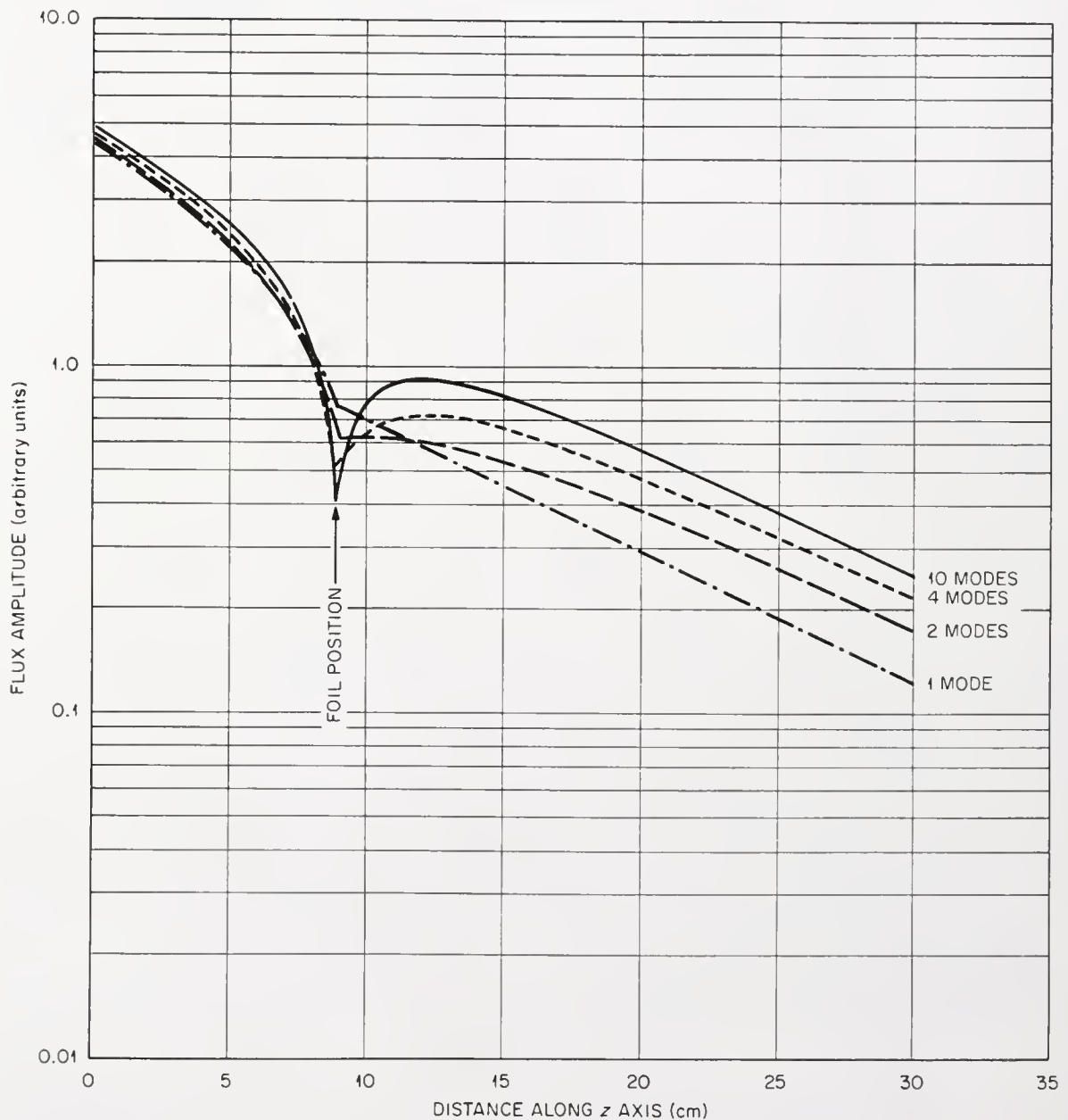


Fig. 2. One-Group Flux Amplitude vs Distance Along the Z Axis for One Cadmium Foil in Graphite, at 100 cps, with 1, 2, 4, and 10 Spatial Modes.

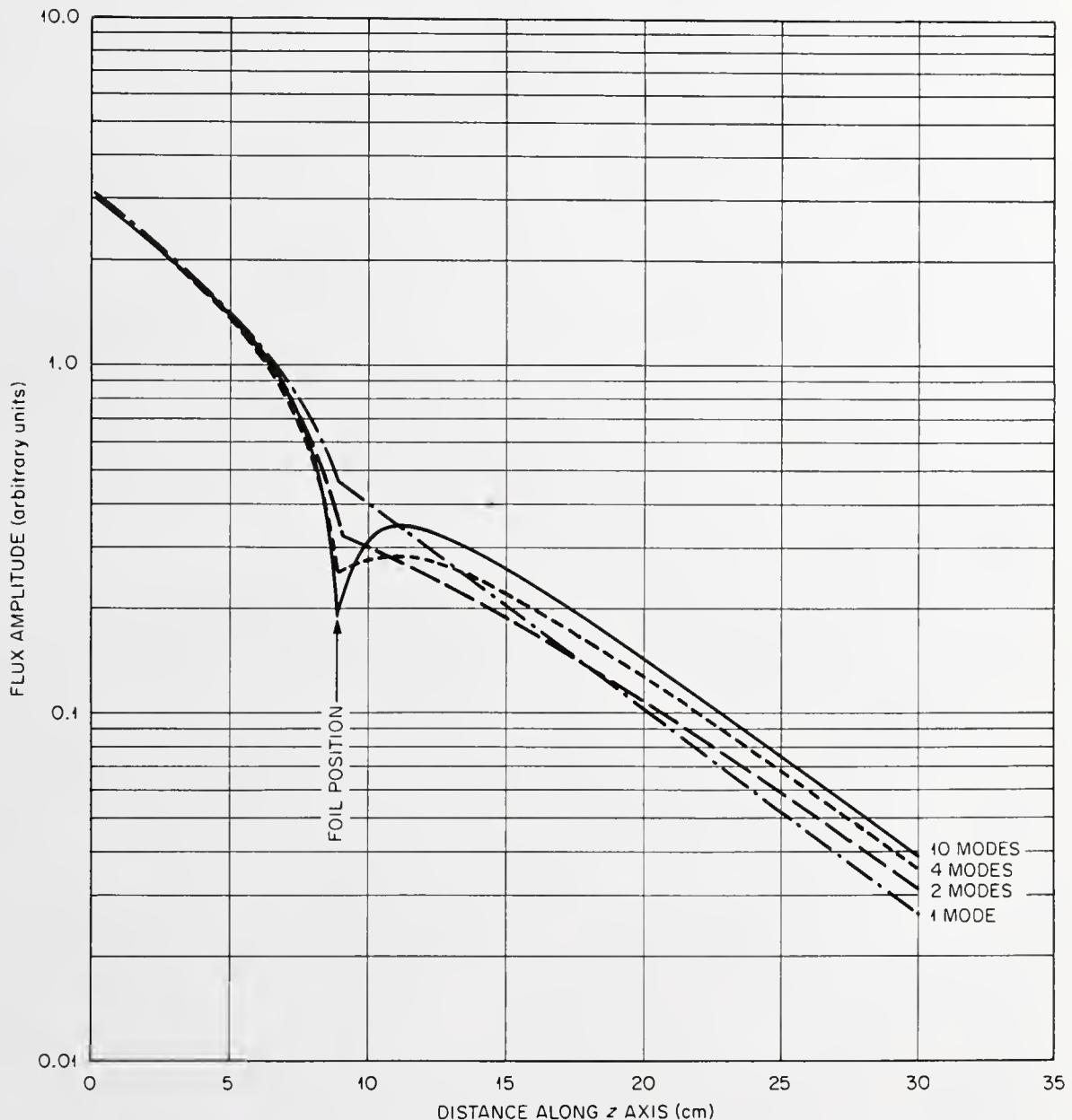


Fig. 3. One-Group Flux Amplitude vs Distance Along the Z Axis for One Cadmium Foil in Graphite, at 1000 cps, with 1, 2, 4, and 10 Spatial Modes.

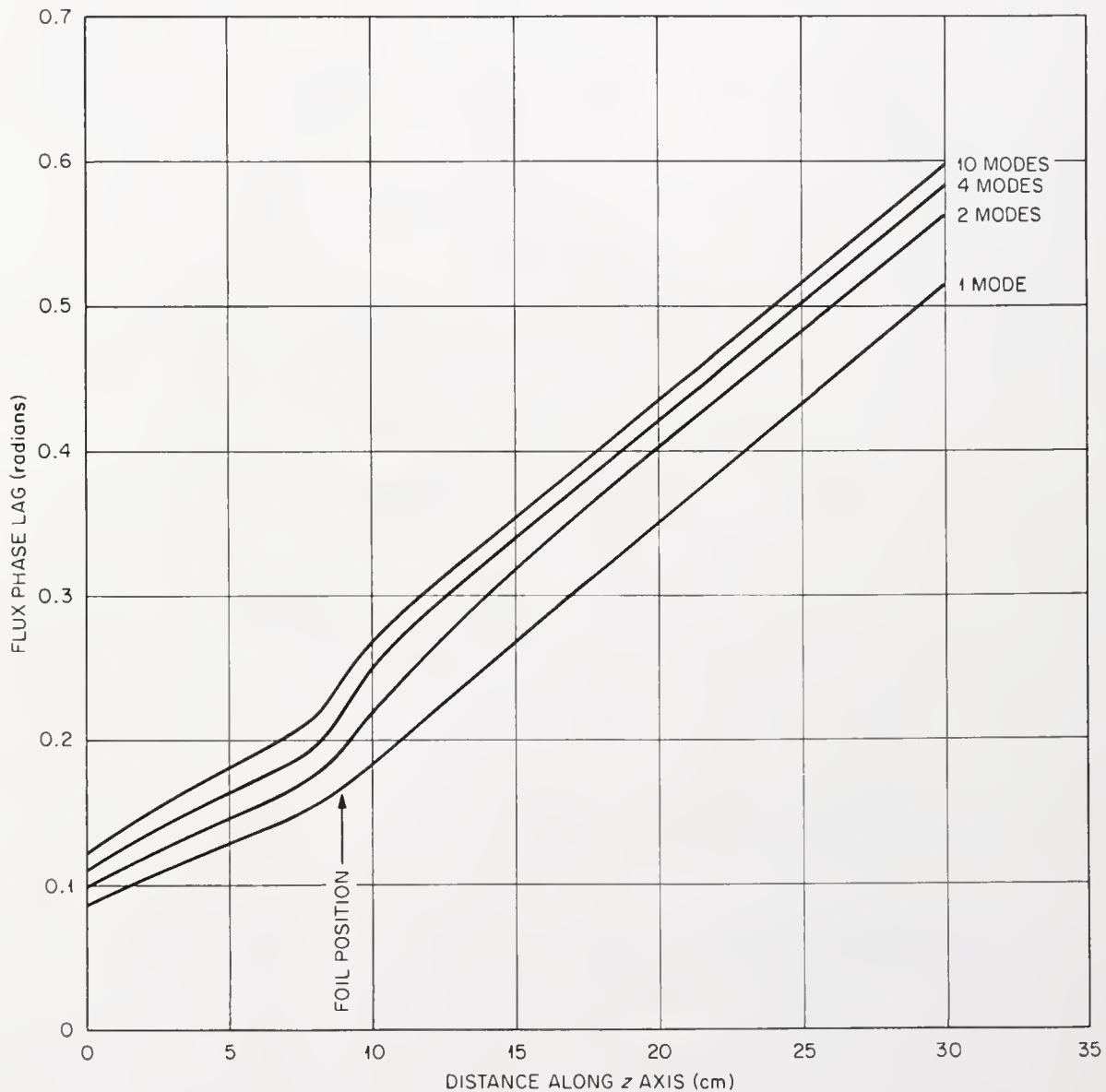


Fig. 4. One-Group Flux Phase Lag vs Distance Along the Z Axis for One Cadmium Foil in Graphite, at 100 cps, with 1, 2, 4, and 10 Spatial Modes.

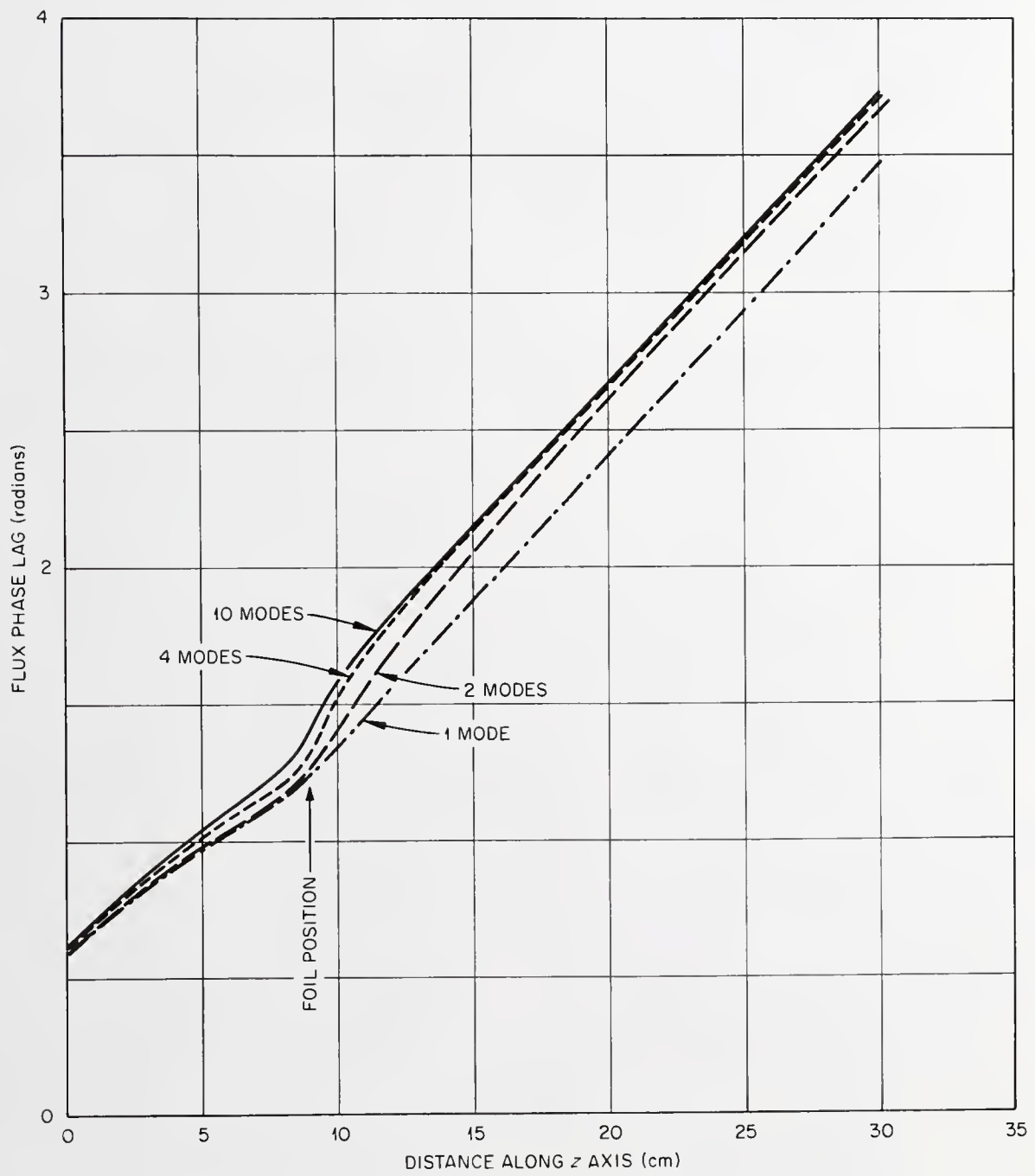


Fig. 5. One-Group Flux Phase Lag vs Distance Along the X Axis for One Cadmium Foil in Graphite, at 1000 cps, with 1, 2, 4, and 10 Spatial Modes.

10 and 8 to 10 modes, respectively. Calculations were limited to 10 spatial modes because of machine storage limitations. Although the convergence is somewhat slow, it is probably adequate for most purposes, especially since the problem used is a rather severe test.

Figures 6-10 show the results of calculations in the same geometry as described above except that two perturbing foils are present, at $z = 8.89$ and 17.78 cm. These foils are either cadmium, as used previously, or U^{235} of the same total absorption cross section as the cadmium strips. The calculations with cadmium are one-group and with U^{235} are age-diffusion. Figure 6 shows flux amplitude as a function of z for one spatial mode calculations using cadmium foils with source frequencies of 200, 500, and 800 cps and using U^{235} foils at 200 cps. The unperturbed flux at 200 cps is also plotted on Fig. 6. Figure 7 shows the same data using six spatial modes. The unperturbed flux is identical in Figs. 6 and 7 since the assembly is driven with fundamental mode only in each case. Figure 8 presents the phase angles as a function of z corresponding to the amplitudes shown in Figs. 6 and 7. The one-group, six-spatial mode calculations shown in Figs. 7 and 8 are replotted as a function of source driving frequency in Figs. 9 and 10. Figure 9 presents flux amplitude versus frequency for z values of 2, 8, 8.89, 15, and 30 cm. Figure 10 presents phase lag for the same conditions.

A second facility that is available at the University of Florida for measurements compatible with the geometry restrictions of these calculations is a water, or D_2O , tank which is 120.97×130.17 cm in the transverse directions. Figure 11 is a plot of flux magnitude versus z at 200 cps for an age-diffusion calculation in D_2O with two 1-in.-diam natural uranium

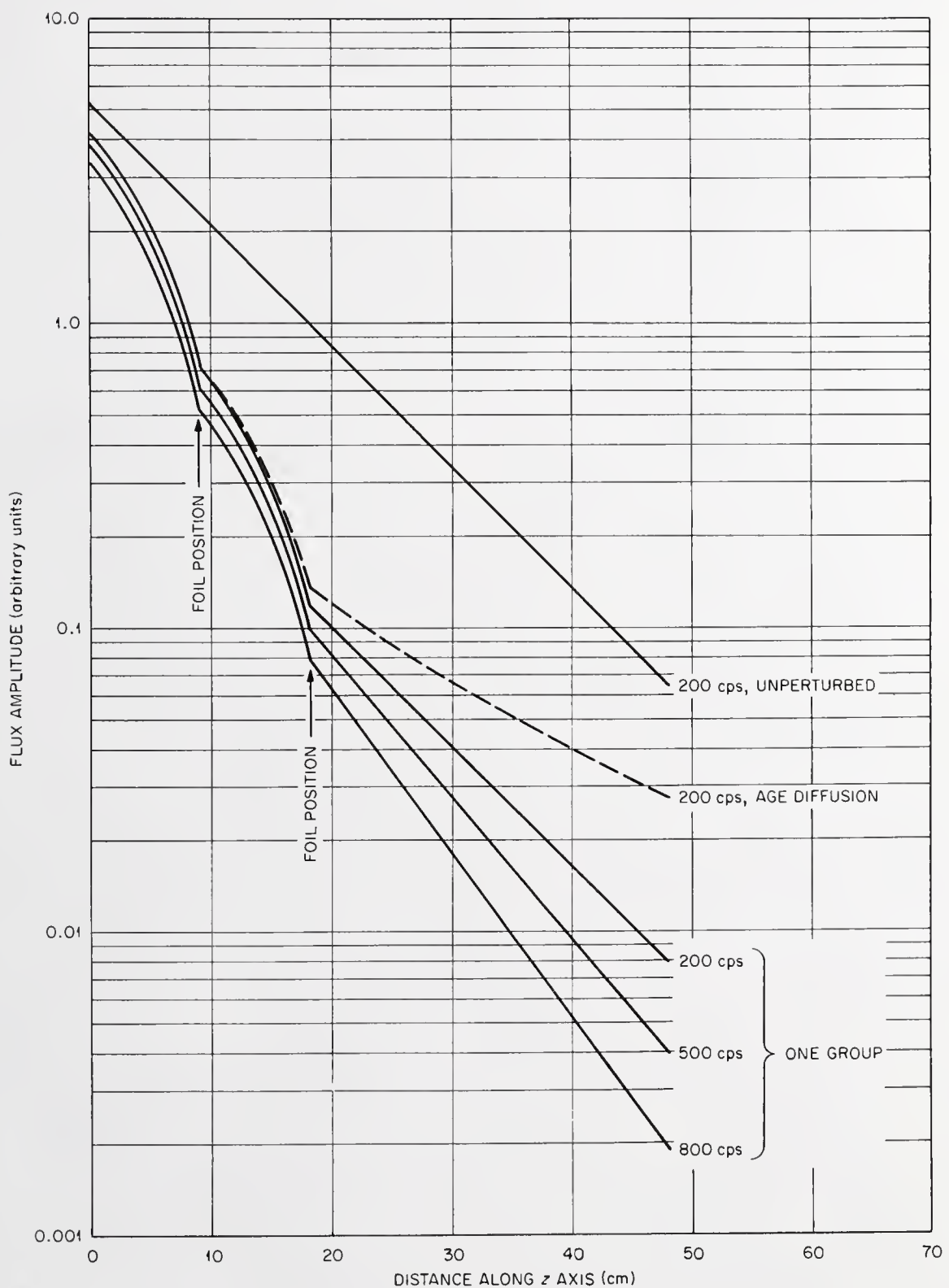


Fig. 6. Flux Amplitude vs Distance Along the Z Axis for Two Cadmium or Uranium Foils in Graphite, at 200, 500, and 800 cps, with One Spatial Mode.

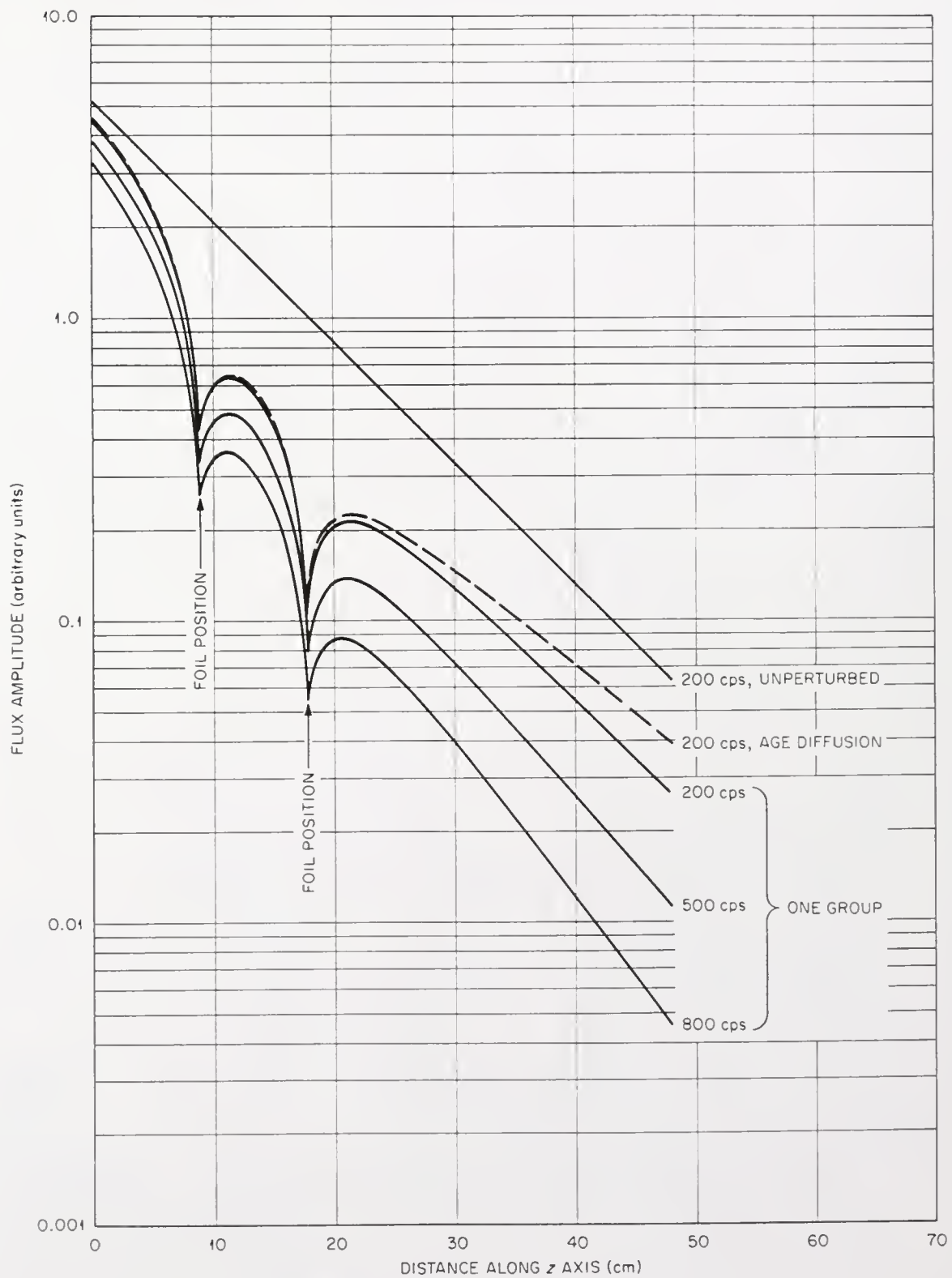


Fig. 7. Flux Amplitude vs Distance Along the Z Axis for Two Cadmium or Uranium Foils in Graphite, at 200, 500, and 800 cps, with Six Spatial Modes.

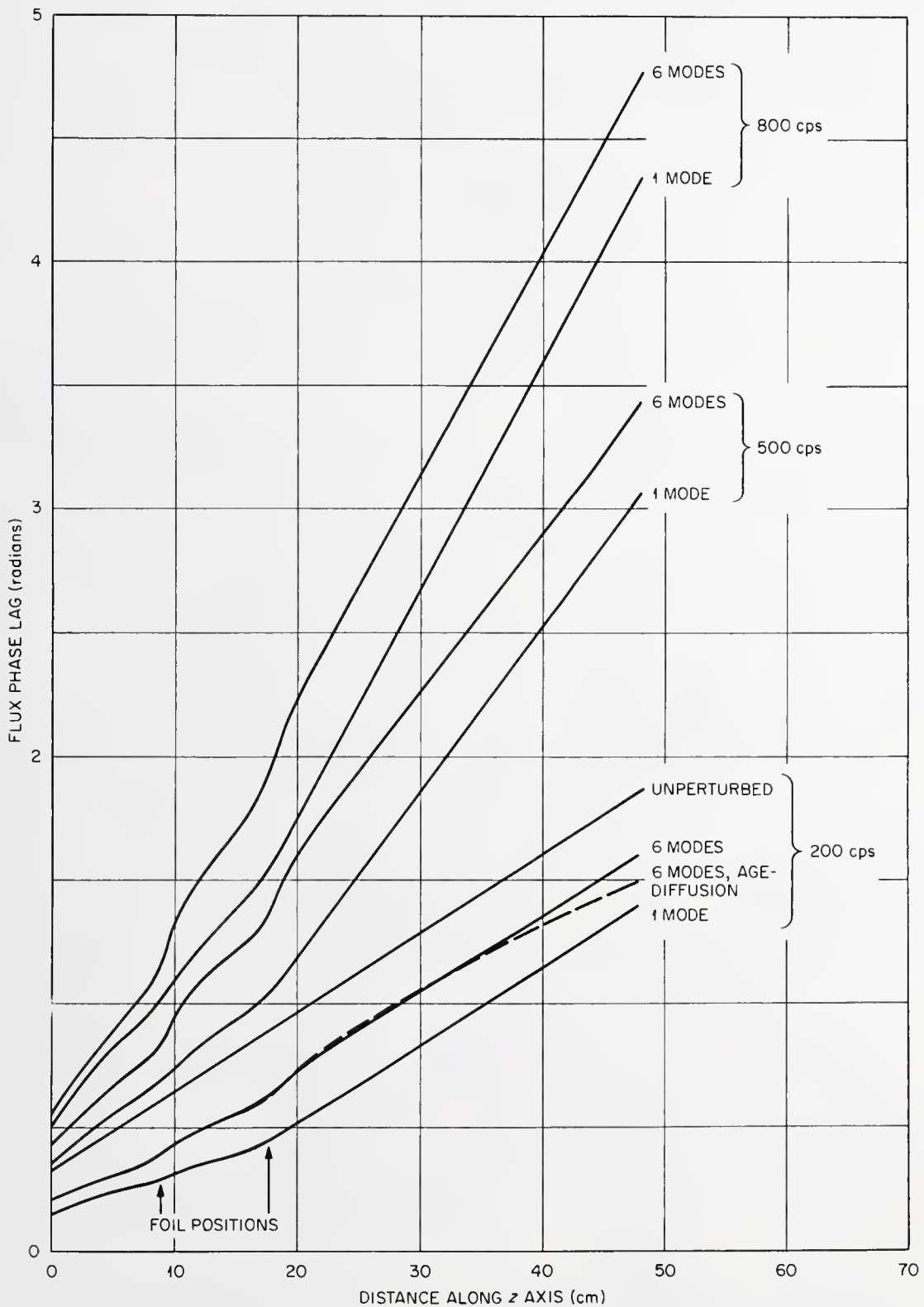


Fig. 8. Flux Phase Lag vs Distance Along the Z Axis for Two Cadmium or Uranium Foils in Graphite, at 200, 500, and 800 cps, with One and Six Spatial Modes.

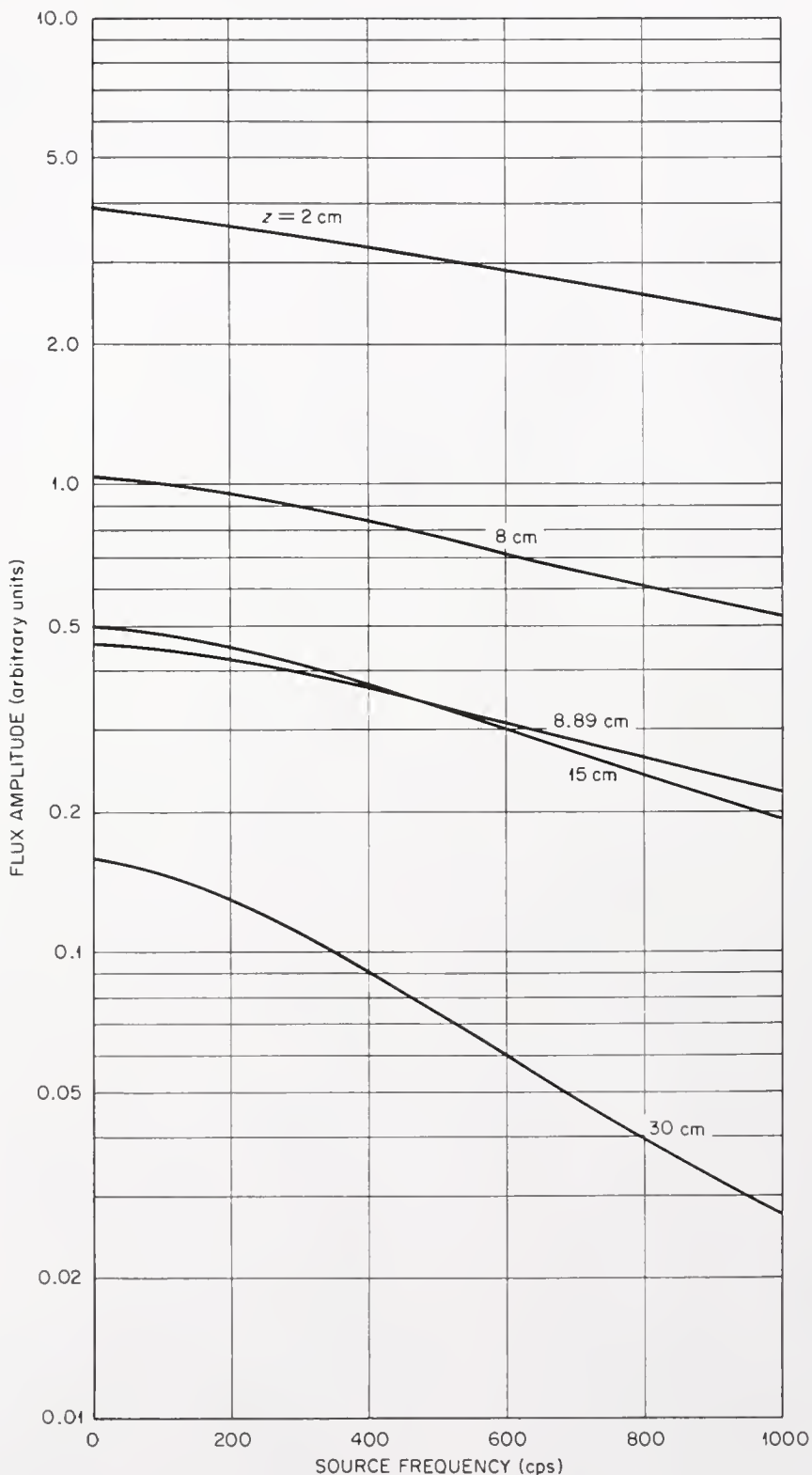


Fig. 9. One-Group Flux Amplitude vs Source Frequency for Two Cadmium Foils in Graphite, at $z = 2, 8, 8.89, 15$, and 30 cm , with Six Spatial Modes.

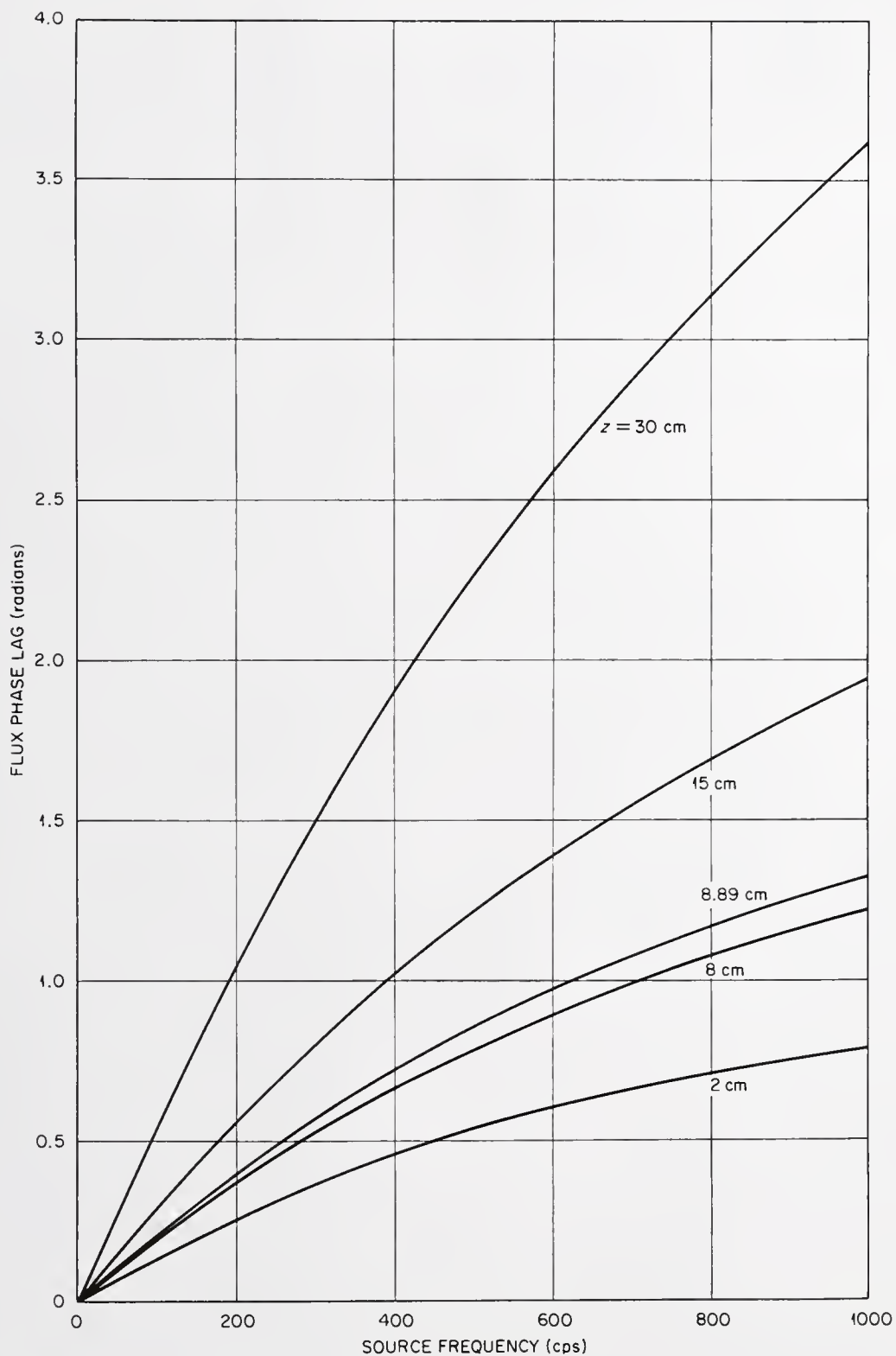


Fig. 10. One-Group Flux Phase Lag vs Source Frequency for Two Cadmium Foils in Graphite, at $z = 2, 8, 8.89, 15$, and 30 cm , with Six Spatial Modes.

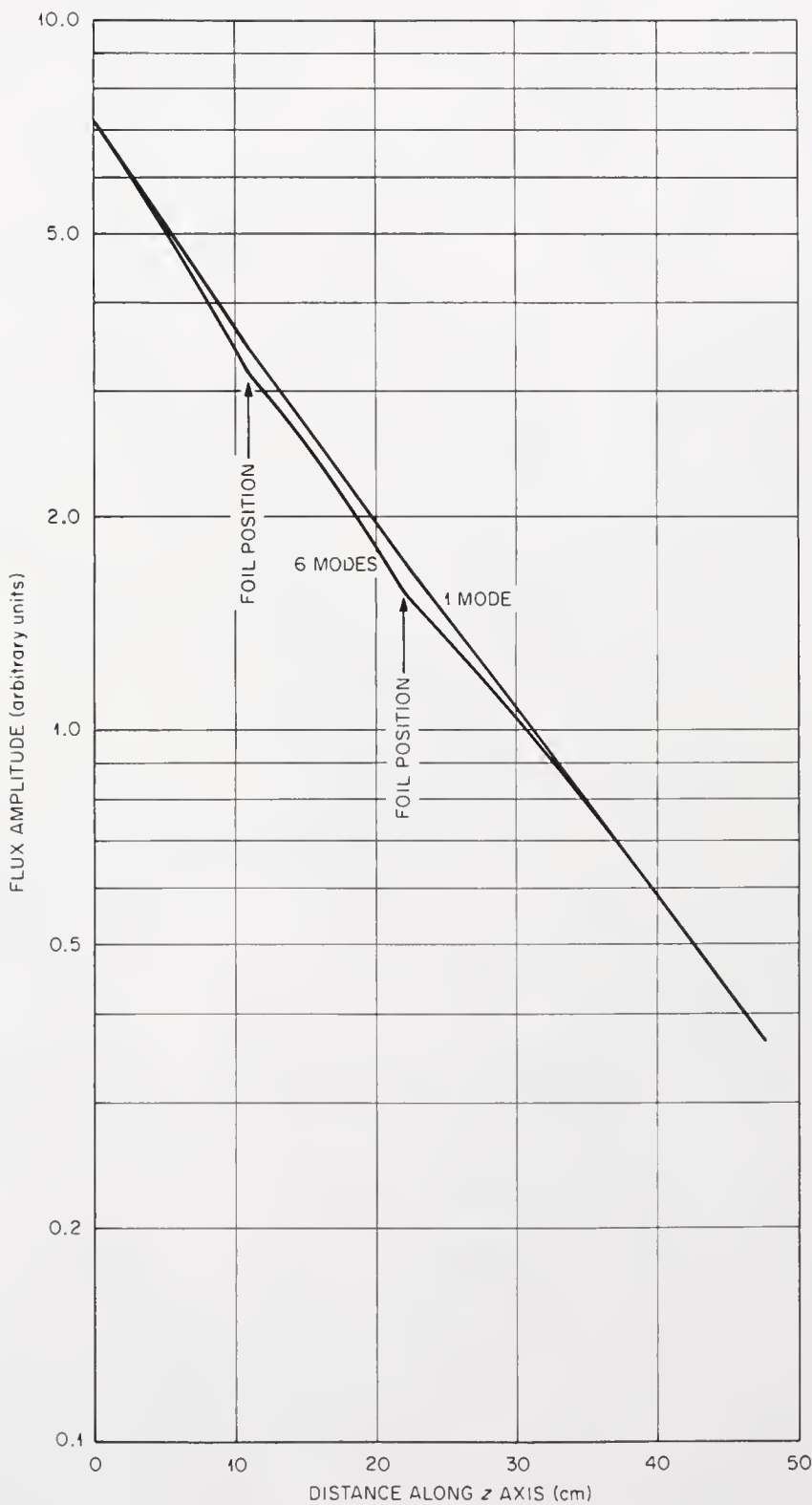


Fig. 11. Age-Diffusion Flux Amplitude vs Distance Along the Z Axis for Two Uranium Foils in D_2O , at 200 cps, with One and Six Spatial Modes.

rods 130.17 cm long located at $z = 10.998$ and 21.996 cm. The obvious characteristic of the calculation is that the natural uranium rods do not offer sufficient perturbation to produce dramatic effects. An alternate and feasible perturbation could be obtained by using single plates from fuel elements of the MTR type. One of these plates has approximately the same total absorption cross section as the natural uranium rods. Therefore, the perturbation would be approximately the same. In order to produce a significant perturbation with fuel, fairly large U^{235} rods would have to be used.

Since the calculation shown in Fig. 11 has small perturbations, it presents a good opportunity to show the relative contributions of the unperturbed, thermal-neutron diffusion, and slowing-down contributions to the final answer. These are shown in Fig. 12, where the three curves correspond to the three terms in Eq. (3.85). Since it is a six-spatial mode calculation, the thermal-neutron diffusion and slowing-down curves are sums of the second and third terms in Eq. (3.85).

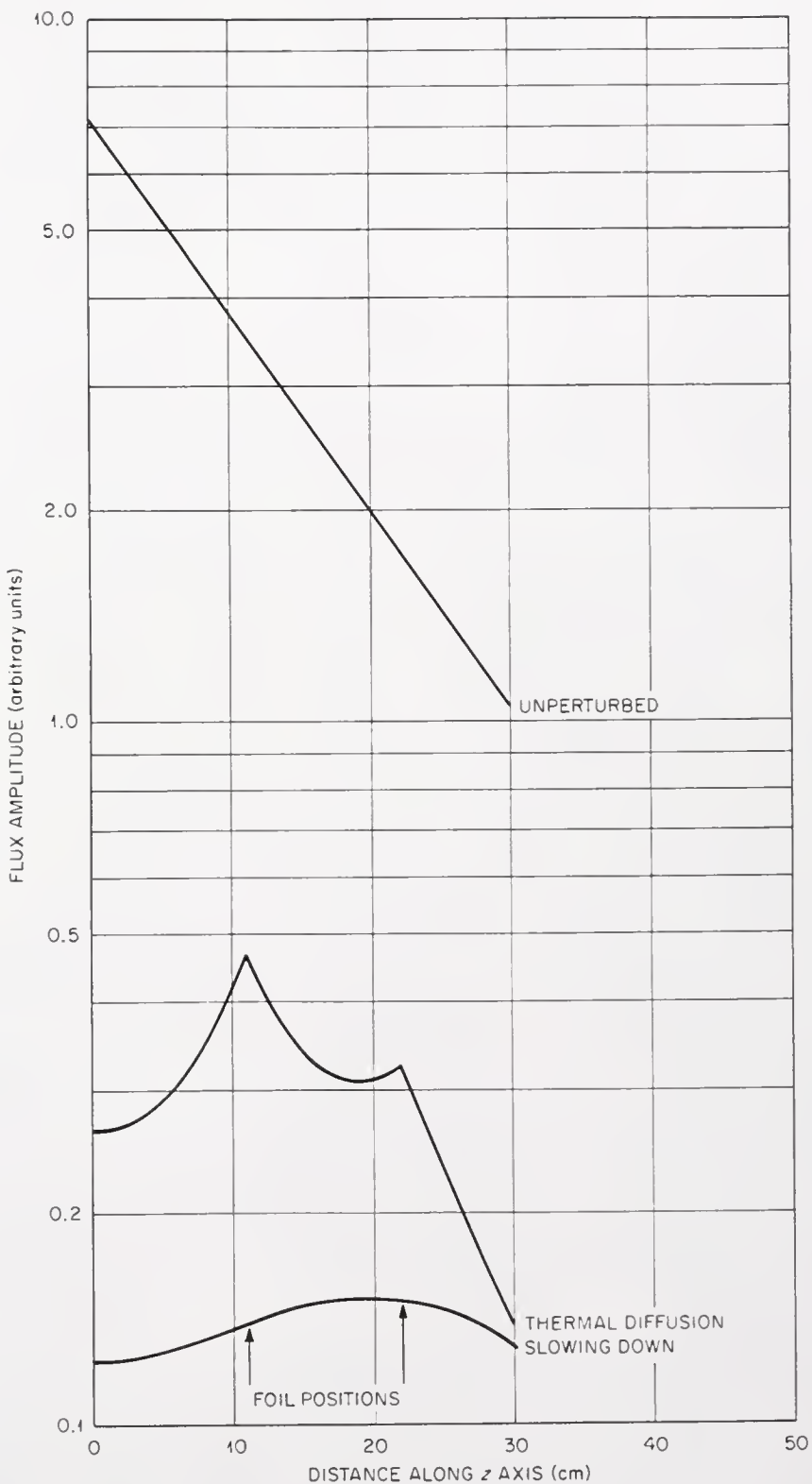


Fig. 12. Components of Age-Diffusion Flux Amplitude *vs* Distance Along the Z Axis for Two Uranium Foils in D_2O , at 200 cps, with Six Spatial Modes.

CHAPTER V

SUMMARY AND CONCLUSIONS

The goal of this dissertation has been to predict, as accurately as possible, the behavior of neutron waves in heterogeneous multiplying and nonmultiplying media. The primary approach has been similar to the heterogeneous reactor theory of Feinberg and Galanin in that the continuous slowing-down model has been assumed to describe the behavior of the neutrons above thermal energy and diffusion theory has been assumed to describe the behavior of the thermal energy neutrons. Rather than assume that the infinite-medium slowing-down and diffusion kernels are applicable, a more basic approach was chosen which resulted in slowing-down and diffusion kernels for the particular finite geometry that was assumed.

The preceding chapter showed some results of calculations using this theory. In this chapter, it will be shown how this theory may be applied and extended.

Application to Critical Reactors

As stated previously, the theoretical developments of this work are, in several ways, an extension of the Feinberg-Galanin heterogeneous reactor theory. Aside from the obvious feature of predicting the behavior of neutron waves in subcritical assemblies, this work takes into account the finiteness of the assembly. The effect that this has is best shown by applying the theory to a critical reactor, which can be done by dropping

the source terms and changing the boundary conditions slightly. The absorptive Green's function defined by Eq. (3.60) will have the same boundary conditions as before except that now $G_j(z, \xi)$ itself, rather than the derivative of $G_j(z, \xi)$, will be required to go to zero at $z = 0$. This change in boundary condition simply results in $G_j(z, \xi)$ changing to

$$G_j(z, \xi) = \frac{e^{-Kz}}{K} \frac{\sinh K\xi}{\xi}, \quad z > \xi, \quad (5.1)$$

$$= \frac{e^{-K\xi}}{K} \frac{\sinh Kz}{z}, \quad z < \xi. \quad (5.2)$$

With the new Green's function, Eq. (3.63) applies to the critical assembly with the added simplification that all the boundary conditions given by the last term in Eq. (3.63) vanish. Equation (3.63) now becomes

$$\phi_{j\ell}(z) = - \sum_k G_j(z_k, z) H_{jk}(z) + A_{\ell j} \sum_k \int_0^\infty d\xi G_j(\xi, z) F_{jk}(\xi, z_k), \quad (5.3)$$

where $G_j(\xi, z)$ is now given by Eqs. (5.1) and (5.2). Remembering that the factors H_{jk} and F_{jk} both contain

$$\phi_\ell(x_k, z_k) = \sum_j \frac{1}{\sqrt{a}} \cos \frac{(2j-1)\pi x_k}{2a} \phi_{j\ell}(z_k), \quad (5.4)$$

it can be seen that, for $k = 1, 2, \dots, M$, and $j = 1, 2, \dots, J$, JM homogeneous equations are available for each value of ℓ . For the system to be critical the determinant of the coefficients of the $\phi_{j\ell}(z_k)$ must be zero. This of course gives an equation which can be solved for η (contained in $A_{\ell j}$) or whatever other eigenvalue is chosen to determine criticality.

The first difference noticed in comparison with the Feinberg-Galanin theory seems to be simply additional complexity since the Feinberg-Galanin theory only requires the solution of an M by M determinant. The improvements are the improved kernels contained in Eq. (5.3). As pointed out in Chapter III, $A_{\ell j}$ and F_{jk} contain the finite-medium slowing-down kernel rather than the infinite-medium kernel used by Feinberg-Galanin. The Green's function G_j also is an improvement, being the finite-medium diffusion kernel for the geometry used in this work, rather than the infinite-medium diffusion kernel used by Feinberg-Galanin.

Conclusions

The theoretical developments of this dissertation probably represent a model which is as complex and physically realistic as is practical at this time. Further improvements, in order to be practical for machine calculations, would certainly be desirable if they simplified the mathematics or if they eliminated remaining physically undesirable assumptions, or both. If such improvements are not easily attainable, the primary question remaining is how to use the theory best to direct future experimental work in this area.

Several approaches are possible. One is simply to continue full calculations of the thermal flux in various configurations, such as those presented in the preceding chapter. This is a rather brute force technique but at least has the advantage that calculations are cheaper and much more easily accomplished than experiments since the machine codes are available. Some possibly more satisfying approaches can be suggested by re-examination of some of the results of Chapter III. To this end, write Eq. (3.64) as

$$\begin{aligned} \phi_{j\ell}(z) &= H_{j\ell} - \frac{1}{D} \sum_k G_j(z, z_k) \frac{\gamma_k}{\sqrt{a}} \cos \frac{(2j-1)\pi x_k}{2a} \phi_\ell(x_k, z_k) \\ &+ E_{\ell j} \sum_k \frac{\gamma_k}{\sqrt{a}} \cos \frac{(2j-1)\pi x_k}{2a} \phi_\ell(x_k, z_k) \int_0^\infty d\xi M_k(\xi) G_j(z_k, \xi) , \end{aligned} \quad (5.5)$$

where

$$H_{j\ell} \equiv - \frac{e^{-Kz}}{K} \left. \frac{d\phi_{j\ell}(\xi)}{d\xi} \right|_{\xi=0} \quad (5.6)$$

and

$$E_{\ell j} \equiv \frac{\Sigma_s(0) \eta p(\tau_s, \omega) e^{-B_{\ell j}^2 \tau_s}}{\Sigma_t(0) 2 D_s} \quad (5.7)$$

and G_j and M_k are defined by Eqs. (3.61) and (3.68), respectively. A corresponding equation exists for $\phi'_{j\ell}(z)$; thus

$$\begin{aligned} \phi'_{j\ell}(z) &= H'_{j\ell} - \frac{1}{D} \sum_k G'_j(z, z_k) \frac{\gamma_k}{\sqrt{a}} \sin \frac{j\pi x_k}{a} \phi_\ell(x_k, z_k) \\ &+ E'_{\ell j} \sum_k \frac{\gamma_k}{\sqrt{a}} \sin \frac{j\pi x_k}{a} \phi_\ell(x_k, z_k) \int_0^\infty d\xi M_k(\xi) G'_j(z_k, \xi) , \end{aligned} \quad (5.8)$$

where G'_j , $H'_{j\ell}$, and $E'_{\ell j}$ are obtained by replacing $B_{\ell j}^2$ with $B'_{\ell j}^2$ and K^2 with K'^2 where they appear in Eqs. (3.61), (5.6), and (5.7), respectively.

Inserting Eqs. (5.5) and (5.8) into Eq. (3.46) and in turn into Eq. (3.17) results in

$$\begin{aligned}
\phi_s(\underline{r}, \omega) = & \sum_{\ell} \frac{1}{\sqrt{b}} \cos \frac{(2\ell - 1)\pi y}{2b} \sum_j \left\{ \frac{1}{\sqrt{a}} \cos \frac{(2j - 1)\pi x}{2a} H_{j\ell} \right. \\
& + \frac{1}{\sqrt{a}} \sin \frac{j\pi x}{a} H'_{j\ell} - \frac{1}{D} \sum_k \left[G_j(z, z_k) C_{jk} \right. \\
& \left. \left. + G'_j(z, z_k) S_{jk} \right] \phi_\ell(x_k, z_k) + E_{\ell j} \sum_k C_{jk} \phi_\ell(x_k, z_k) \right. \\
& \left. \int_0^\infty d\xi M_k(\xi) G_j(z_k, \xi) + E'_{\ell j} \sum_k S_{jk} \phi_\ell(x_k, z_k) \int_0^\infty d\xi M_k(\xi) G'_j(z_k, \xi) \right\} ,
\end{aligned} \tag{5.9}$$

where

$$C_{jk} \equiv \frac{\gamma_k}{a} \cos \frac{(2j - 1)\pi x_k}{2a} \cos \frac{(2j - 1)\pi x_k}{2a} \tag{5.10}$$

and

$$S_{jk} \equiv \frac{\gamma_k}{a} \sin \frac{j\pi x}{a} \sin \frac{j\pi x_k}{a} . \tag{5.11}$$

Experimental measurements of thermal neutron flux as a function of position and frequency represent the quantity calculated in Eq. (5.9). These data may be operated on with

$$\int_{-a}^a dx \cos \frac{(2j - 1)\pi x}{2a} \int_{-b}^b dy \cos \frac{(2\ell - 1)\pi y}{2b} \tag{5.12}$$

or with

$$\int_{-a}^a dx \sin \frac{j\pi x}{a} \int_{-b}^b dy \cos \frac{(2\ell - 1)\pi y}{2b} \tag{5.13}$$

to yield experimental measurements of the flux components calculated, respectively, in Eqs. (5.5) and (5.8). This entire procedure may be performed experimentally with the moderator alone, with fuel plates or rods and with purely absorbing plates or rods of the same macroscopic absorbing cross section as the fuel assemblies. The technique of replacing fuel assemblies with comparable pure absorbers has been utilized previously to measure effective delayed neutron fractions (11). The six terms in Eqs. (5.5) and (5.8) may now be separated. The homogeneous experiment yields $H_{j\ell}$ and $H'_{j\ell}$. Subtracting the homogeneous term from the pure-absorber data yields the absorption terms, the second terms in Eqs. (5.5) and (5.8). Similarly, the difference between the pure absorber and the fuel assembly data yields the last terms which contain the slowing-down kernels.

Since the above experimental data would presumably be obtained by cadmium-difference measurements with a neutron detector which has approximately a $1/v$ response, it is also of interest to calculate the epicadmium flux or cadmium-covered detector response. Equation (3.44) may be rewritten as

$$Q_\ell(x, z, \tau) = \frac{\Sigma_s(0)}{\Sigma_t(0)} \frac{n}{2} \sum_j \sum_k M_k(z, \tau) \left[e^{-B_{\ell j}^2 \tau} C_{jk} + e^{-B_{\ell j}^{\prime 2} \tau} S_{jk} \right] \phi_\ell(x_k, z_k) . \quad (5.14)$$

The argument τ has been added to M_k as a reminder that M_k is defined as in Eq. (3.68) except that τ replaces τ_s . Insertion of Eqs. (5.14) into Eq. (3.18) yields

$$q(\underline{r}, \tau) = p(\tau, \omega) \sum_{\ell} \frac{1}{\sqrt{b}} \cos \frac{(2\ell - 1)\pi y}{2b} \frac{\Sigma_s(0)}{\Sigma_t(0)} \frac{n}{2}$$

$$\sum_j \sum_k M_k(z, \tau) \left[e^{-B_{\ell j}^2 \tau} C_{jk} + e^{-B_{\ell j}'^2 \tau} S_{jk} \right] \phi_{\ell}(x_k, z_k) . \quad (5.15)$$

The response of the $1/v$ detector covered with cadmium can be taken to be proportional to

$$\begin{aligned} \psi_{epi}(\underline{r}, \omega) &= \sqrt{\frac{2E_0}{m}} \int_0^{u_{cd}} q(\underline{r}, \tau) \frac{1}{v} du \\ &= \int_0^{u_{cd}} q(\underline{r}, \tau) e^{u/2} du , \end{aligned} \quad (5.16)$$

where u_{cd} is the lethargy of the cadmium cutoff. Insertion of Eq. (5.15) into Eq. (5.16) gives

$$\begin{aligned} \psi_{epi}(\underline{r}, \omega) &= \sum_{\ell} \frac{1}{\sqrt{b}} \cos \frac{(2\ell - 1)\pi y}{2b} \frac{\Sigma_s(0)}{\Sigma_t(0)} \frac{n}{2} \\ &\sum_j \sum_k \left[I_{\ell j k} C_{jk} + I'_{\ell j k} S_{jk} \right] \phi_{\ell}(x_k, z_k) , \end{aligned} \quad (5.17)$$

where

$$I_{\ell j k} \equiv \int_0^{u_{cd}} p(u, \omega) M_k(z, u) e^{-B_{\ell j}^2 u} e^{u/2} du \quad (5.18)$$

and

$$I'_{\ell jk} = \int_0^{u_{cd}} p(u, \omega) M_k(z, u) e^{-B_{\ell j}^2 u} e^{u/2} du . \quad (5.19)$$

As before, experimental measurements of the quantity represented by Eq. (5.17) taken as a function of position and frequency may be operated on with the operators given in Eqs. (5.12) and (5.13). Let the result of operating with Eq. (5.12) on Eq. (5.17) be called $F_{\ell jk}$, which is

$$F_{\ell jk} = \frac{\Sigma_s(0)}{\Sigma_t(0)} \frac{1}{2} \sum_k I'_{\ell jk} \frac{\gamma_k}{\sqrt{a}} \cos \frac{(2j - 1)\pi x_k}{2a} \phi_{\ell}(x_k, z_k) . \quad (5.20)$$

The nonsymmetric part may be called $F'_{\ell jk}$ and is obtained by operating with Eq. (5.13) on Eq. (5.17), giving

$$F'_{\ell jk} = \frac{\Sigma_s(0)}{\Sigma_t(0)} \frac{1}{2} \sum_k I'_{\ell jk} \frac{\gamma_k}{\sqrt{a}} \sin \frac{j\pi x_k}{a} \phi_{\ell}(x_k, z_k) . \quad (5.21)$$

Several things should be noted at this point. First, all the information obtained thus far could have been obtained from experimental data taken at only one z value. Secondly, each term obtained experimentally except for the homogeneous term has contained a weighted summation over the thermal neutron flux at the surface of the foils. Alternatively, by combining the thermal constant, γ_k , with the flux, these summations may be considered to include the net current into each of the foils.

Assume now that the experimental data and following analysis have been performed for M values of z , different from the locations of the M foils, of course. These M values of z should be chosen so as to be fairly close to the M foil locations in order to maximize the information about

the foils in the M sets of measurements. Now assume that this set of information is available for the symmetric absorption term, the second term in Eq. (5.5). A set of M inhomogeneous equations results, with the M unknowns being the net current into each of the M foils or, if γ_k is known, being the surface flux at each of the M foils.

Now that the net current into each foil is known, this information may be inserted into some of the other terms to obtain additional information. For instance, having the net currents and experimental values of $F_{\ell jk}$ at M points, the integrals $I_{\ell jk}$ defined in Eq. (5.18) may be obtained by solving the set of M equations given by Eq. (5.20). Alternatively, if the $E_{\ell j}$'s are assumed to be known, the integrals over the slowing-down kernel in Eq. (5.5) may be obtained for each foil.

APPENDIX A

THE COMPLEX ARITHMETIC VERSION OF GINV

GINV is a FORTRAN subroutine developed by Burrus et al. (12) for the purpose of obtaining working inverses to singular matrices or to matrices which appear singular to a digital computer. It was modified to handle complex arithmetic and was used in the programs employed for calculations in this dissertation because, at one point, it appeared that the matrices in these problems were very ill conditioned. Although this turned out not to be the case, it was left in because it takes up little more storage than a standard matrix inverter and gives slightly better answers in practically all situations.

Theoretically, the inverse of a matrix A , A^{-1} , has the property that $A^{-1} A = I$, where I is the identity matrix. This property never is true precisely, when an inverse is obtained on a digital computer with finite accuracy. GINV operates so as to find the working inverse A^W , defined as that matrix for which the root mean square value of $(I - A^W A)$ is a minimum.

The theory of operation will not be given here since it is not pertinent to this dissertation and should be available soon in the literature (13).

Pages 90-92 contain the FORTRAN listing of the program as modified for complex arithmetic. Sufficient comment cards are included to enable a competent programmer to modify the program for ordinary FORTRAN arithmetic.

A few comments may be appropriate on the use of the program. First, when TAU is set to zero, the routine performs virtually the same operations as other matrix inverters and should give identical results on well-conditioned matrices. It may also be noted that if the problem to be solved is to obtain x from $Ax = b$, where A is an $m \times n$ matrix (with $n < m$) and b is a given m component vector, GINV automatically obtains the least-squares solution to the set of n equations. It is obviously much more versatile than most matrix routines, although its full versatility was not needed in this work.

SUBROUTINE GINV(A,MR,NR,NC,TAU,U,ATEMP)

UPON ENTRY A = A MATRIX WITH NR ROWS AND NC COLUMNS
AFTER THE RETURN THE ORIGINAL A IS DESTROYED AND THE
ARRAY A CONTAINS THE TRANSPOSE OF T, THE TRANSFORMATION
MATRIX (X = T*B) WHICH SOLVES THE PAIR OF EQUATIONS

A*X = B AND TAU I*X = 0

IN THE LEAST SQUARE SENSE.

MR = 1ST DIM. NO. OF ARRAY A IN THE CALLING PROGRAMS
TAU IS A NON-NEGATIVE CONSTANT WHICH CONTROLS THE ERROR
PROPAGATION OF THE TRANSFORMATION MATRIX. IF TAU = 0.
THEN THE RESULTING TRANSFORMATION MATRIX IS THE
ORDINARY LEAST SQUARES TRANSFORMATION MATRIX.

(THE INVERSE IF NR = NC)

ATEMP AND U ARE USED FOR WORKING SPACE BY THE ALGORITHM
AND DO NOT NECESSARILY CONTAIN ANY RELEVANT NUMBERS AT
THE CONCLUSION. ATEMP MUST BE DIMENSIONED AT LEAST NC
BY THE CALLING PROGRAMS. U MUST BE DIMENSIONED AT
LEAST NC*NC BY THE CALLING PROGRAMS.

NO. OF MULTIPLICATIONS = NC**2 (5/2 NR + 2/3 NC)

I DIMENSION A(30,30), U(30,30), ATEMP(30), DOT(1),
I DUT2(1), TAUSQ(1), DUM(1)

C THE DIM. ST. AS SENT BY ROSS BURRUS FOR FORTRAN IV WAS
C DIMENSION A(MR,NC),U(NC,NC),ATEMP(NC)

C NOTE THAT IN COMPLEX ARITHMETIC VERSION, IT HAS BEEN
C ASSUMED THAT MR IS ALSO THE 2ND DIM. NO. OF A AS WELL
C AS THE 1ST.

TAUSQ(1) = TAU**2

TAUSQ(2) = 0.0

PLACE UNIT MATRIX IN U

DO 5 I = 1,NC

 DO 4 J = 1,NC

I 4 U(I,J) = (0.0,0.0)

I 5 U(I,I) =(1.0,0.0)

```

C      ORTHOGONALIZE COMBINED MATRIX (A ABOVE U) BY GRAMM-
C      SCHMIDT-HILBERT METHOD WITH FIRST NR ROWS WEIGHTED
C      WITH 1 AND THE OTHER NC ROWS WEIGHTED WITH 1/TAU.  THEN
C      REORTHOGONALIZE TO LESSEN ROUNDOFF ERROR.
C
C      DO 20 I = 1,NC
C             IMR = I + MR
C             II = I - 1
C             IF (II) 2,11,2
C 2      DO 10 LL = 1,2
C             DO 10 J = 1,II
C                 JMR = J+MR
C
C                 DOT =(0.0,0.0)
C                 DOT2 =(0.0,0.0)
C                 DO 3 K = 1,NR
C                     DUM(1) = A(K,J)
C                     DUM(2) = -A(K,JMR)
C 3             DOT = A(K,I)*DUM + DOT
C
C
C             DO 6 K = 1,J
C                 DUM(1) = U(K,J)
C                 DUM(2) = -U(K,JMR)
C 6             DOT2 = U(K,I)*DUM + DOT2
C             DOT = DOT + DOT2*TAUSQ
C             DO 8 K = 1,J
C                 U(K,I) = U(K,I) - DOT*U(K,J)
C 8             DO 10 K = 1,NR
C                 A(K,I) = A(K,I) - DOT*A(K,J)
C
C      NORMALIZE THE COLUMN I OF THE COMBINED MATRIX
C
C 11      DOT =(0.0,0.0)
C 12      DOT2 =(0.0,0.0)
C 13      DO 12 K = 1,NR
C             DOT = DOT + A(K,I)**2 + A(K,IMR)**2
C 14      DO 14 K = 1,I
C             DOT2 = DOT2 + U(K,I)**2 + U(K,IMR)**2
C             DOT = DOT + DOT2*TAUSQ
C             DOT = SQRTE(DOT)
C 15      DO 17 K = 1,I
C             U(K,I) = U(K,I)/DOT
C 16      DO 19 K = 1,NR
C             A(K,I) = A(K,I)/DOT
C 20      CONTINUE

```

C CALCULATION OF THE TRANSPOSE OF THE TRANSFORMATION
C MATRIX T(TRANS.) = A * U(TR.)
C
I DO 50 I = 1,NR
I DO 45 J = 1,NC
I ATEMP(J) =(0.0,0.0)
I DO 45 K = J,NC
I KMR = K+MR
I DUM(1) = A(I,K)
I DUM(2) = -A(I,KMR)
I ATEMP(J) = DUM*U(J,K) + ATEM(J)
I 45 CONTINUE
I DO 50 J = 1,NC
I A(I,J) = ATEM(J)
I CONTINUE
50 RETURN
END

APPENDIX B

DIGITAL COMPUTER TECHNIQUES FOR THE CALCULATION OF THE ERROR FUNCTION WITH A COMPLEX ARGUMENT

The calculation of the error function with a complex argument is a problem which arose some time ago in heat flow theory (14). Two infinite series approximations (accurate to 1 part in 10^{16}) are derived in a paper by Salzer (15) and two rather simple formulas, valid for large arguments, are given by Gautschi (16). Two of the above techniques have been incorporated into computer subroutines that are believed to give accuracies of at least 1 part in 10^6 over virtually the entire region of the complex plane which can be handled by a 36-bit digital computer, such as the International Business Machine (IBM) 709.

Since Salzer covers the derivation of the infinite series approximations quite thoroughly, only a brief introduction to the development, to illustrate the complexity of the problem, will be given. The ordinary error function is usually defined as

$$\text{erf}(x) \equiv \frac{2}{\sqrt{\pi}} \int_0^x e^{-t^2} dt . \quad (\text{B.1})$$

When the complex argument is introduced, the integration must proceed along some line in the complex plane. If the integration goes from the point $(0,0)$ to the point (X,Y) , one such possible path is from O to X along the real axis, then vertically from $(X,0)$ to (X,Y) . This results in

$$\operatorname{erf}(X + iY) \equiv \frac{2}{\sqrt{\pi}} \int_0^{X+iY} e^{-z^2} dz = \frac{2}{\sqrt{\pi}} \int_0^X e^{-x^2} dx + \frac{2i}{\sqrt{\pi}} \int_0^Y e^{-(X+iy)^2} dy . \quad (\text{B.2})$$

The first integral may be recognized as $\operatorname{erf}(X)$, and further manipulation with the second integral gives

$$\operatorname{erf}(X + iY) = \operatorname{erf}(X) + \frac{2e^{-X^2}}{\sqrt{\pi}} \left\{ \int_0^Y e^{y^2} \sin 2XY dy + i \int_0^Y e^{y^2} \cos 2XY dy \right\} . \quad (\text{B.3})$$

The two integrals in Eq. (B.3) must be performed numerically. The very clever technique described by Salzer results in infinite series approximations to the two functions in the integrals, each term of which can be integrated to give infinite series approximations to the two integrals, which are accurate to 1 part in 10^{16} . The result is

$$\begin{aligned} \operatorname{erf}(X + iY) &= \operatorname{erf}(X) + \frac{e^{-X^2}}{2\pi X} [(1 - \cos 2XY) + i \sin 2XY] \\ &+ \frac{2e^{-X^2}}{\pi} \sum_{n=1}^{\infty} \frac{e^{-n^2/4}}{n^2 + 4X^2} [F_n(X, Y) + i g_n(X, Y)] + \epsilon(X, Y) , \end{aligned} \quad (\text{B.4})$$

where

$$F_n(X, Y) = 2X - 2X \cosh nY \cos 2XY + n \sinh nY \sin 2XY \quad (\text{B.5})$$

and

$$g_n(X, Y) = 2X \cosh nY \sin 2XY + n \sinh nY \cos 2XY , \quad (\text{B.6})$$

and the error term is approximately

$$|\epsilon(x, y)| \leq 10^{-16} |\operatorname{erf}(x + iy)| . \quad (\text{B.7})$$

The two formulas given by Gautschi are

$$w(z) = iz \left[\frac{0.4613135}{z^2 - 0.1901635} + \frac{0.09999216}{z^2 - 1.7844927} + \frac{0.002883894}{z^2 - 5.5253437} \right] + \epsilon(z) , \quad (\text{B.8})$$

where

$$z = x + iy , \quad (\text{B.9})$$

$$w(z) \equiv e^{-z^2} \left[1 + \frac{2i}{\sqrt{\pi}} \int_0^z e^{t^2} dt \right] = e^{-z^2} \operatorname{erfc}(-iz) , \quad (\text{B.10})$$

$$\operatorname{erfc}(z) = 1 - \operatorname{erf}(z) , \quad (\text{B.11})$$

$$|\epsilon(z)| < 2 \times 10^{-6} \text{ for } x > 3.9 \text{ or } y > 3 , \quad (\text{B.12})$$

and

$$w(z) = iz \left[\frac{0.5124242}{z^2 - 0.2752551} + \frac{0.05176536}{z^2 - 2.724745} \right] + \eta(z) , \quad (\text{B.13})$$

with

$$|\eta(z)| < 10^{-6} \text{ for } x > 6 \text{ or } y > 6 . \quad (\text{B.14})$$

Equations (B.4), (B.8), (B.10), and (B.13) are all valid over the entire complex plane, but Eq. (B.10) must be handled carefully to obtain $\operatorname{erf}(z)$ in terms of $w(z)$. Using the property

$$w(\bar{z}) = \overline{w(-z)} , \quad (B.15)$$

where the bar indicates the complement, and Eq. (B.11), Eq. (B.10) may be manipulated to obtain an expression valid for $x > 0$ and $y > 0$:

$$\operatorname{erf}(z) = 1 - e^{y^2-x^2} (\cos 2xy - i \sin 2xy) \overline{w(y+ix)} . \quad (B.16)$$

Using Eq. (B.16) to perform calculations in the first quadrant of the complex plane, the symmetry properties of the error function can be used to reach the other three quadrants. Defining

$$z \equiv x + iy , \quad (B.17)$$

$$\bar{z} \equiv x - iy , \quad (B.18)$$

$$\underline{z} \equiv -x + iy , \quad (B.19)$$

the error function has the following properties:

$$\operatorname{erf}(-z) = -\operatorname{erf}(z) , \quad (B.20)$$

$$\operatorname{erf}(\bar{z}) = \overline{\operatorname{erf}(z)} , \quad (B.21)$$

$$\operatorname{erf}(\underline{z}) = \underline{\operatorname{erf}(z)} . \quad (B.22)$$

Figure 13 shows the various regions of the complex plane when different techniques were used to calculate the error function. In Region I, defined by $|x| < 9.38$ and $|y| < 9.38$, Eqs. (B.4), (B.5), and (B.6) were used. In order to obtain an accuracy of 1 part in 10^8 , it was found necessary to use approximately $9 + 2|y|$ terms in Eq. (B.4). In Region II, defined by $y^2 - x^2 < -88.028$, the error function is $(1,0)$ for $x > 0$ and

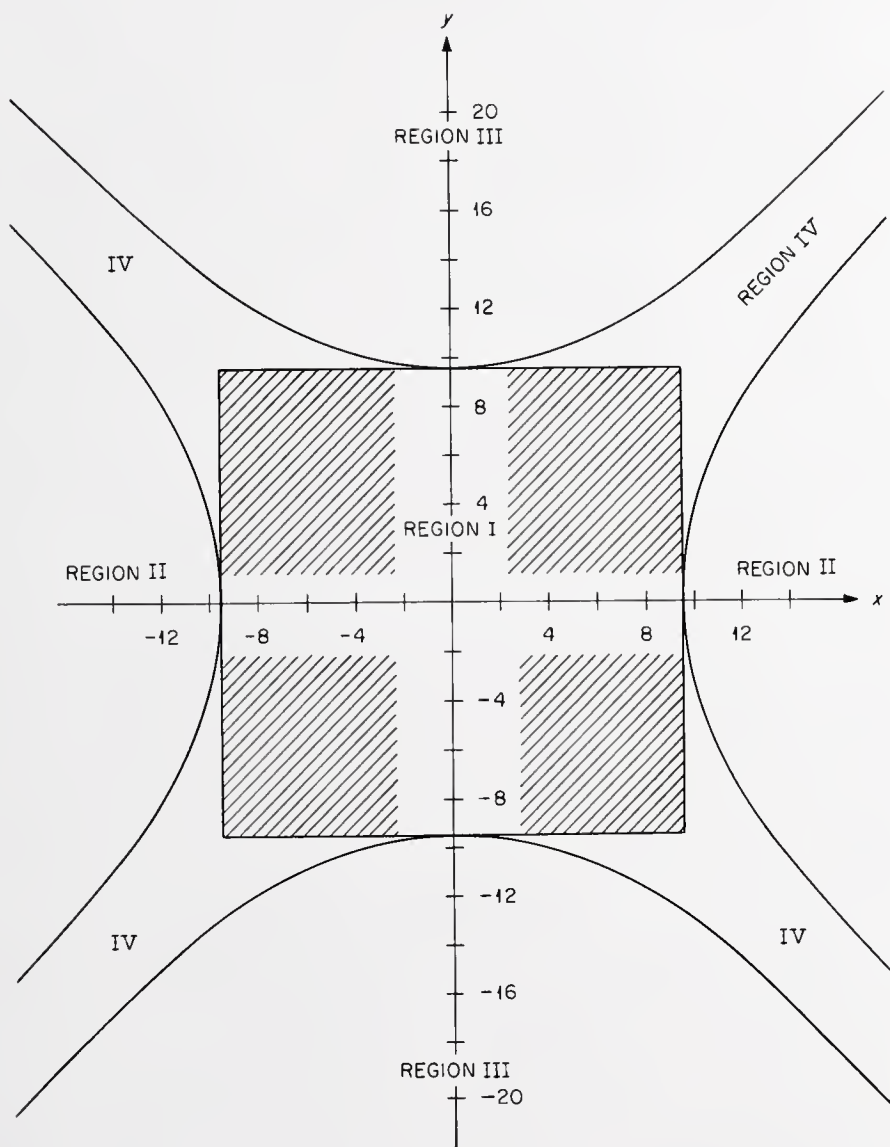


Fig. 13. Regions of Complex Plane Requiring Different Techniques for Calculating the Error Function.

is $(-1,0)$ for $x < 0$, to the numerical limits of an IBM 709 or similar computer. In Region III, defined by $y^2 - x^2 > 88.027$, the imaginary part (and sometimes also the real part) of the error function exceeds the capacity of an IBM 709 and therefore cannot be calculated. Region IV is defined by the remaining four portions of the complex plane, and in this area Eqs. (B.13) and (B.16) were used.

The following two pages give FORTRAN listings of the two computer subroutines. SUBROUTINE CMERFN is entered initially. If $|x| < 9.38$ and $|y| < 9.38$, it uses Eqs. (B.4), (B.5), and (B.6) to perform the calculation and then returns. This calculation takes a considerable amount of machine time, the measured running times for the IBM 709 being approximately 0.15 sec for 11 terms and 0.34 sec for 28 terms. If x or y is outside Region I of Fig. B.1, CMERFN transfers control to SUBROUTINE ERFGR6. ERFGR6 gives an error return if it finds that the point is in Region III, and uses Eqs. (B.13) and (B.16) and the symmetry properties for Regions II and IV.

It may be noted that ERFGR6 is a rather straightforward conversion of the appropriate equations to FORTRAN statements, but it was found necessary to reformulate Eqs. (B.4), (B.5), and (B.6) slightly for CMERFN in order to cover the full range of y values. The form used was obtained by expressing the hyperbolic functions in Eqs. (B.5) and (B.6) in terms of exponentials, then combining these exponentials with the factor $\exp(-n^2/4)$. Another noteworthy feature of this subroutine is that it uses four terms of the Maclaurin series for the terms $(1 - \cos 2xy)/x$ and $(\sin 2xy)/x$ when $|xy| < 0.1$, rather than using the FORTRAN SIN and COS functions. This feature was found to be necessary to ensure 8-digit accuracy for the complete region.

```

SUBROUTINE CMERFN (X,Y,REERFN,CMER,N)
C FOR ABSF(X) AND ABSF(Y) LESS THAN 9.38, THIS ROUTINE USES
C UP TO 28 TERMS OF A SERIES TO CALCULATE THE ERF(X+IY).
C OUTSIDE THIS RANGE, IT CALLS ERFGR6.
N=0
IF (ABSF(X)-9.38) 10,10,15
10 IF (ABSF(Y)-9.38) 25,25,15
15 CALL ERFGR6(X,Y,REERFN,CMER)
RETURN
25 CONS = .636619772
C CONS = 2/PI
CONS = CONS/EXP(1.0)
ERFUFX = ERFF(X)
TWOX = 2.0*X
COS2XY = CUSF (TWOX*Y)
SIN2XY = SINF (TWOX*Y)
IF (ABSF(X*Y)-0.1) 50,50,75
50 XY2 = X*X*Y*Y
A = X*Y*Y*(.5-XY2/6.*(.1-XY2/7.5*(1.-XY2/14.1)))
B = Y*(.5-XY2/3.*(.1-XY2/5.*(.1-XY2/10.5)))
GO TO 100
75 A = (1.0-COS2XY)/2./TWOX
B = SIN2XY/2./TWOX
100 N = N+1
IF (N-30) 125,125,175
175 REERFN = ERFUFX + CONS*A
CMER = CONS*B
WRITE OUTPUT TAPE 6,150,N,REERFN,CMER,AERR,BERR,X,Y
150 FORMAT (I10,6E18.9)
RETURN
125 FN = FLOAT(N)
FNY = FN*Y
DUMY=1./(FN**2+TWOX**2)
255 EXPP = EXP(FN*(Y-FN/4.))/2.
EXPN = EXP(-FN*(Y+FN/4.))/2.
ADUM=EXPP*(FN*SIN2XY-TWOX*COS2XY)
1 -EXPN*(FN*SIN2XY+TWOX*COS2XY)
2 +TWOX*EXP(-FN*FN/4.)
BDUM=EXPP*(FN*COS2XY+TWOX*SIN2XY)
1 -EXPN*(FN*COS2XY-TWOX*SIN2XY)
275 ADUM = DUMY*ADUM
BDUM = DUMY*BDUM
AERR = ADUM/A
BERR = BDUM/B
A = A+ADUM
B = B+BDUM
300 IF (ABSF(AERR) + ABSF(BERR) - 1.E-8) 200,200,100
200 CONTINUE
REERFN= ERFUFX + CONS*A
CMER = CONS*B
RETURN
END

```

```

      SUBROUTINE ERFGR6(X,Y,Z1,Z2)
C  IF Y**2-X**2 IS GREATER THAN 88.027, AN ERROR RETURN IS
C  GIVEN.  IF Y**2-X**2 IS LESS THAN -88.028, IT SHOULD
C  RETURN SIGNF(1.0,X) AS Z1 AND ZERO AS Z2.
I   DIMENSION Z(1),G(1)
I   IF(Y*Y-X*X-88.027) 5,5,3
3   WRITE OUTPUT TAPE 6,4,X,Y
4   FORMAT (29H CMERFN UNABLE TO HANDLE X =E20.9,
2      9H OR Y =E20.9)
      RETURN
I   5 A = (0.5124242,0.)
I   B = (0.2752551,0.)
I   C = (0.05176536,0.)
I   D = (2.724745,0.)
      SX = SIGNF(1.0,X)
      SY = SIGNF(1.0,Y)
      X = ABSF(X)
      Y = ABSF(Y)
      Z(1) = Y
      Z(2) = X
I   G = Z*Z
I   Z = A/(G-B) + C/(G-D)
      G(1) = -X
      G(2) = Y
I   Z = G*Z
      Z(2) = -Z(2)
      LX = EXPF(Y*Y-X*X)
      G(1) = EX*COSF(2.*X*Y)
      G(2) = -EX*SINF(2.*X*Y)
I   7 A = (+1.0,0.0)
I   8 Z = A - G*Z
      Z1 = Z(1)*SX
      Z2 = Z(2)*SY
      RETURN
      END

```

APPENDIX C

GALANIN'S THERMAL CONSTANT FOR A SINUSOIDALLY VARYING FLUX

The thermal constant, γ , defined by Feinberg and Galanin as the ratio of the net current into a small slug or foil to the neutron flux on its surface, is a real constant in the steady-state case. It is fairly easy to show that γ becomes complex when the flux is varying sinusoidally. If diffusion theory is applicable in the slug, it is evident that the factor $1/L^2$ in the usual diffusion equation must be replaced by $1/L^2 + i \omega/vD$.

Using diffusion theory, Galanin (17) obtains the following formulas. For an infinite cylinder of radius ρ ,

$$\gamma = \frac{2\pi\rho D}{L} \frac{I_1(\rho/L)}{I_0(\rho/L)} , \quad (C.1)$$

where D and L are the diffusion coefficient and diffusion length in the foil, and I_0 and I_1 are modified Bessel functions of the first kind. For an infinite slab of thickness $2d$,

$$\gamma = \frac{2D}{L \coth \left(\frac{d}{L} \right)} . \quad (C.2)$$

It should be noted that the above equation includes a factor of 2 which was left out of Galanin's formula (36.2).

The above formulas are applicable for the present work simply by making the substitution noted above for L, if one is willing to make the assumptions of diffusion theory and infinite dimensions of the fuel slugs or foils. More elaborate calculations are certainly feasible although somewhat involved.

APPENDIX D

PHYSICAL CONSTANTS USED IN SAMPLE CALCULATIONS

In order to permit reproduction of the sample calculations of Chapter IV, the physical constants which were used are given below:

<u>Parameter</u>	<u>Graphite</u>	<u>Heavy Water (99.5% D₂O)</u>
p (τ_s)	0.93	0.999
T _s	1.47×10^{-4}	5.08×10^{-5}
τ_s	364.	125.
Σ_a	4.09×10^{-4}	1.37×10^{-4}
D	0.986	0.823

p (τ_s) and T_s are defined in Eqs. (4.3) and (4.5). τ_s is the Fermi age to thermal, in cm², as defined by Eq. (3.11). Σ_a and D are defined in Eq. (1.1).

The thermal constant, γ , was taken to be 7.8232 for the cadmium foils and 0.3227 for the uranium foils. η for uranium was taken to be 2.07.

REFERENCES

1. R. B. Perez and R. E. Uhrig, Nuclear Sci. Eng. 17, 90-100 (1963).
2. R. H. Hartley, Master's Thesis, University of Florida, 1964.
3. R. S. Booth, Ph.D. Dissertation, University of Florida, 1965.
4. R. B. Perez and R. S. Booth, Proceedings of the Symposium on Pulsed Neutron Research, Karlsruhe, Germany, 1965 (to be published).
5. R. S. Booth, private communication.
6. R. S. Denning et al., Trans. Am. Nucl. Soc. 7, 229 (1964).
7. A. D. Galanin, Proc. Intern. Conf. Peaceful Uses At. Energy, Geneva, 1955 5, 462-465 (1955).
8. S. M. Feinberg, Proc. Intern. Conf. Peaceful Uses At. Energy, Geneva, 1955 5, 484-500 (1955).
9. P. M. Morse and H. Feshbach, Methods of Theoretical Physics, Part II, McGraw-Hill, New York, 1953.
10. J. H. Dunlap, University of Florida, private communication.
11. R. Perez-Belles et al., Nucl. Sci. Eng. 12, 505-512 (1962).
12. W. R. Burrus et al., Neutron Physics Division Annual Progress Report for Period Ending August 1, 1964, ORNL-3714 (1), pp. 74-77.
13. C. Schneeberger and W. R. Burrus, Application of an Algorithm for the Generalized Inverse to Linear Equations (unpublished ORNL report).
14. S. Whitehead, Proc. Phys. Soc. (London) 56(6), 357-366 (1944).
15. H. E. Salzer, Math. Tables Aids Comp. 5, 67-70 (1951).

16. M. Abramowitz and I. E. Stegun (eds.), Handbook of Mathematical Functions with Formulas, Graphs, and Mathematical Tables, Natl. Bur. Std. (U.S.) Applied Math Series 55, 328 (1964).
17. A. D. Galanin, Thermal Reactor Theory, Pergamon, New York, 1960.

BIOGRAPHICAL SKETCH

Victor Ralph Cain was born August 31, 1934, in Carter, Oklahoma. In June 1952, he was graduated from Norman High School. In August 1956, he received the degree of Bachelor of Science in Engineering Physics from the University of Oklahoma. In 1956 he joined the staff of Oak Ridge National Laboratory in Oak Ridge, Tennessee. From 1957 until 1963 he attended the Graduate School at the University of Tennessee where he received the degree of Master of Science in August 1963. In September 1963, he was assigned by Oak Ridge National Laboratory to work toward the Ph.D. degree at the University of Florida.

Victor Ralph Cain is married to the former Patricia Ann Lamb and is the father of four children. He is a member of Phi Eta Sigma, Tau Beta Pi and the American Nuclear Society.

This dissertation was prepared under the direction of the chairman of the candidate's supervisory committee and has been approved by all members of that committee. It was submitted to the Dean of the College of Engineering and to the Graduate Council, and was approved as partial fulfillment of the requirements for the degree of Doctor of Philosophy.

August 14, 1965

R Martin
Dean, College of Engineering

Dean, Graduate School

Supervisory Committee:

Rafael R. Lin
Chairman

Robert E. Sheng
J. S. Chanian

Reyrefide
A. R. Quinton

3202 A
25